Simulating spatio-temporal dynamics of surface $PM_{2.5}$ emitted from Alaskan wildfires

Dong Chen (itscd@umd.edu)*[a], Michael Billmire (mgbillmi@mtu.edu)[b], Christopher P. Loughner (christopher.loughner@noaa.gov)[c], Allison Bredder (bredder@umd.edu)[a], Nancy H.F. French (nhfrench@mtu.edu)[b], Hyun Cheol Kim (hyun.kim@noaa.gov)[c,d], Tatiana V. Loboda (loboda@umd.edu)[a]

[a] Department of Geographical Sciences, University of Maryland, College Park, Maryland, USA

[b] Michigan Tech Research Institute, Michigan Technological University, Ann Arbor, Michigan, USA

[c] Air Resources Laboratory, National Oceanic and Atmospheric Administration, College Park, Maryland, USA

[d] Cooperative Institute for Satellite Earth System Studies, University of Maryland, College Park, Maryland, USA

*Corresponding author.

Abstract

Wildfire is a major disturbance agent in Arctic boreal and tundra ecosystems that emits large quantities of atmospheric pollutants, including PM2.5. Under the substantial Arctic warming which is two to three times of global average, wildfire regimes in the high northern latitude regions are expected to intensify. This imposes a considerable threat to the health of the people residing in the Arctic regions. Alaska, as the northernmost state of the US, has a sizable rural population whose access to healthcare is greatly limited by a lack of transportation and telecommunication infrastructure and low accessibility. Unfortunately, there are only a few air quality monitoring stations across the state of Alaska, and the air quality of most remote Alaskan communities is not being systematically monitored, which hinders our understanding of the relationship between wildfire emissions and human health within these communities. Models simulating the dispersion of pollutants emitted by wildfires can be extremely valuable for providing spatially comprehensive air quality estimates in areas such as Alaska where the monitoring station network is sparse. In this study, we established a methodological framework that is based on an integration of the Hybrid Single-Particle Lagrangian Integrated Trajectory (HYSPLIT) model, the Wildland Fire Emissions Inventory System (WFEIS), and the Arctic-

Boreal Vulnerability Experiment (ABoVE) Wildfire Date of Burning (WDoB) dataset, an Arctic-oriented fire product. Through our framework, daily gridded surface-level PM2.5 concentrations for the entire state of Alaska between 2001 and 2015 for which wildfires are responsible can be estimated. This product reveals the spatio-temporal patterns of the impacts of wildfires on the regional air quality in Alaska, which, in turn, offers a direct line of evidence indicating that wildfire is the dominant driver of PM2.5 concentrations over Alaska during the fire season. Additionally, it provides critical data inputs for research on understanding how wildfires affect human health which creates the basis for the development of effective and efficient mitigation efforts.

Keywords:
Air pollution, $PM_{2.5}$, HYSPLIT, remote sensing, boreal forests, wildfire, biomass burning, Alaska

1. Introduction

Wildfires, both of natural and anthropogenic origins, occur in a wide variety of ecosystems around the world (Jolly et al., 2015). In addition to imposing strong impacts on the carbon cycle (Balshi et al., 2009; Gibson et al., 2018), energy budget (Randerson et al., 2006), hydrological cycle (Shakesby and Doerr, 2006), and causing substantial economic losses (Gill et al., 2013), wildfires are also known to be a major threat to public health. Wildfires emit a range of gaseous and particulate pollutants in high quantities, including PM2.5 (particulate matter with a diameter of 2.5 μm or less) (Matz et al., 2020; Naeher et al., 2007; Sullivan et al., 2008). Typically resulting from incomplete combustion and condensation of combustion gases (Naeher et al., 2007), PM2.5 is a pollutant with potent toxicity and has been shown to be associated with a wide array of negative health outcomes, including asthma (Fan et al., 2016; Hahn et al., 2021), lung cancer (Wei et al., 2017), coronary heart disease (Hu, 2009), premature death (Kloog et al., 2013), diabetes (Chen et al., 2013), and adverse birth outcomes (Kloog et al., 2012).

Wildfires are the major disturbance agent in circumpolar boreal forests (Kasischke and Turetsky, 2006) and tundra (Hu et al., 2015) - the two northernmost biomes on Earth. Over the past decades, temperatures in these two biomes have increased at alarming rates that are two to three times the global average (AMAP, 2021; Schuur et al., 2015). One of the consequences of

such substantial warming is an intensification of the wildfire regimes, particularly within boreal forests (Balshi et al., 2009; Flannigan et al., 2005; Stocks et al., 1998). Boreal wildfires are a major emitter of pollutants for two main reasons. First, the median size of wildfires is generally larger in boreal forests than in temperate forests in North America (Chen et al., 2021a). Even though more than half of global boreal forests are considered under a certain level of management, because of their vast expanse and remote nature, active fire suppression is not implemented in most of boreal forests except for a few regions where boreal forests border relatively densely-populated areas, such as southern Canada and Fennoscandia (Gauthier et al., 2015; Melvin et al., 2017; Parisien et al., 2020). Consequently, many boreal wildfires fall under the "let burn" policy, allowing many of them to burn through large pieces of land. Second, boreal wildfires are pervasive. They are an intrinsic part of the ecological succession of boreal tree species (Johnstone and Chapin, 2006; Taylor and Chen, 2011). Their role in boreal forest ecosystems is so crucial that the boreal forest region is a mosaic of forest stands of different ages, successional stages, and stature shaped by wildfires (Erni et al., 2018; Gromtsev, 2002; Macias Fauria and Johnson, 2008; Weir et al., 2000). In Alaska, 75 % of burned areas since the 1940s are located in boreal forests, according to our calculation based on the Alaska Large Fire Database (ALFD) and the World Wide Fund (WWF) Terrestrial Ecoregions dataset (Olson et al., 2001). Because of the large size and pervasiveness of boreal wildfires, boreal wildfires consume large quantities of biomass, which, in turn, leads to substantial releases of PM2.5 (Ikeda and Tanimoto, 2015; Sapkota et al., 2005).

Fire-driven PM2.5 emissions are a major contributor to poor air quality events throughout the fire season, which nominally lasts between May and September, although the majority of burning usually occurs between early June and the end of August (Abatzoglou and Kolden, 2011; Grabinski and McFarland, 2020). The conventional approach to monitoring air pollution, which relies on surface policy-grade air quality monitoring stations, is extremely limited in Alaska. There are fewer than 30 Environmental Protection Agency (EPA)-grade stations for the entire state and most of them are located within urban environments (according to EPA's website: https://www.epa.gov/o utdoor-air-quality-data). Alaska is sparsely populated with only two urbanized areas (i.e., those above the 50,000 population threshold) and an additional 13 urban clusters (i.e., 2500–49,999 population) (Alaska Department of Transportation and Public Facilities, 2022). About a third of the Alaskan population resides in rural areas (U.S. Department

of Agriculture, 2019) and many of them live in remote communities with limited access to health care (Goldsmith, 2008; Hahn et al., 2021; HRSA, 2021). Surface station-based monitoring provides an extremely limited view of air quality for the state as a whole and is not representative of conditions outside large urban centers. Expanding the network of policy-grade (e.g., EPA-grade) or even low-cost air quality stations, such as PurpleAir (https://www2.purpleair.com/), to achieve an appropriate level of air quality assessment coverage for rural populations would be prohibitively expensive and their maintenance would be unfeasible. It is, therefore, crucial to develop PM2.5 modeling approaches that can deliver air quality assessment across Alaska as a whole, irrespective of population distribution.

While health studies have investigated the impact of health outcomes and specific pollutants (e.g., ozone), they often focus on human exposure to the mix of pollutants constituting a certain size, with PM2.5 being common (Alexeeff et al., 2021; Anderson et al., 2012; Atkinson et al., 2014; Chen and Hoek, 2020; Xing et al., 2016). In retrospective health studies, PM2.5 datasets are commonly linked to patient hospitalization records both temporally and spatially for exposure assessment (Sun et al., 2010; Zhu et al., 2020). The exposure datasets and spatio-temporal matching techniques used to assign an individual's exposure with health outcomes in air pollution studies varies by study objective and design. However, earlier studies generally used coarser resolution (e.g., city-level) data from point source monitors to assign exposure. Now, the standard practice in exposure assessment is to use datasets derived from advanced computer modeling techniques that incorporate Earth observations from satellites (Chen and Hoek, 2020; Diao et al., 2019). The type of gridded PM2.5 concentration map presented in this study can help the community understand spatio-temporal trends of air pollution. In particular, air pollution concentrations can be used in retrospective health studies to understand the health impacts of exposure to air pollution (Anderson et al., 2012; Hahn et al., 2021), allowing for a more accurate estimate of spatiotemporal exposure of an entire population, which, in turn, allows for estimation of both short and long-term effects (Manisalidis et al., 2020).

A common approach for delivering gridded PM2.5 concentration estimates for areas outside existing air quality monitoring networks relies on inputs from Earth-observing satellites. Specifically, the relationship between surface-measured PM2.5 concentrations and, most frequently, satellite-based estimates of aerosol optical depth (AOD) and auxiliary meteorological and other spatially explicit information is identified through the application of statistical models

and, subsequently, extrapolated over the remaining areas. However, the extreme paucity of monitoring stations and their placement in highly selective areas substantially limits the predictive power of such statistical relationships.

Over much of Alaska, anthropogenic sources of PM2.5 emissions are overall scarce (except for a few communities adjacent to major highways and gas/oil production sites, as shown in Fig. 1), which means wildfire smoke is likely the dominant source of PM2.5 for Alaska's rural communities during the fire season. Based on this hypothesis, we further hypothesize that modeling the cumulative emission and transport of PM2.5 from all known wildfires presents a viable option for estimating the PM2.5 concentrations at a state level. In recent years, a few research efforts have been taken to model the transport of wildfire smoke and the resultant dispersion of PM2.5, including the BlueSky smoke modeling framework (Larkin et al., 2009), the National Oceanic and Atmospheric Administration's (NOAA) Smoke Forecasting System (SFS) (Rolph et al., 2009), the University of Alaska Fairbanks smoke forecast system (UAFSmoke) (Grell et al., 2011), the High-Resolution Rapid Refresh- Smoke (HRRR-Smoke) model (Ahmadov et al., 2017), and most recently the HYSPLIT-based Emissions Inverse Modeling System for wildfires (HEIMS-fire) (Kim et al., 2020). While all these smoke modeling systems cover Alaska to different degrees, all of them are operation-based with the goal to provide smoke forecasts over a certain period of time into the future. As a result, their historical model runs have not been maintained to allow for being used in retrospective health analyses (with the exception of HRRR-Smoke, which is being systematically archived by the University of Utah, however, Alaska is excluded from the archive). The FireWork (Pavlovic et al., 2016) model is another smoke forecasting system produced by Environment and Climate Change Canada and the Canadian Forest Service. None of the above smoke forecasting systems are suitable to analyze spatial and temporal trends covering an extended time period throughout Alaska. This highlights a need for a systematically produced, gridded surface-level PM2.5 concentration dataset that covers a relatively long period of time (to be coupled with long-term public health data). In this study, utilizing a state-of-the-art fire emission system, coupled with an atmospheric transport model, the Hybrid Single-Particle Lagrangian Integrated Trajectory (HYSPLIT) model (Draxler and Hess, 1998; Stein et al., 2015), we developed a system where the atmospheric concentrations of PM2.5 that are attributable to wildfires were estimated for the entire state of Alaska over 15 years.

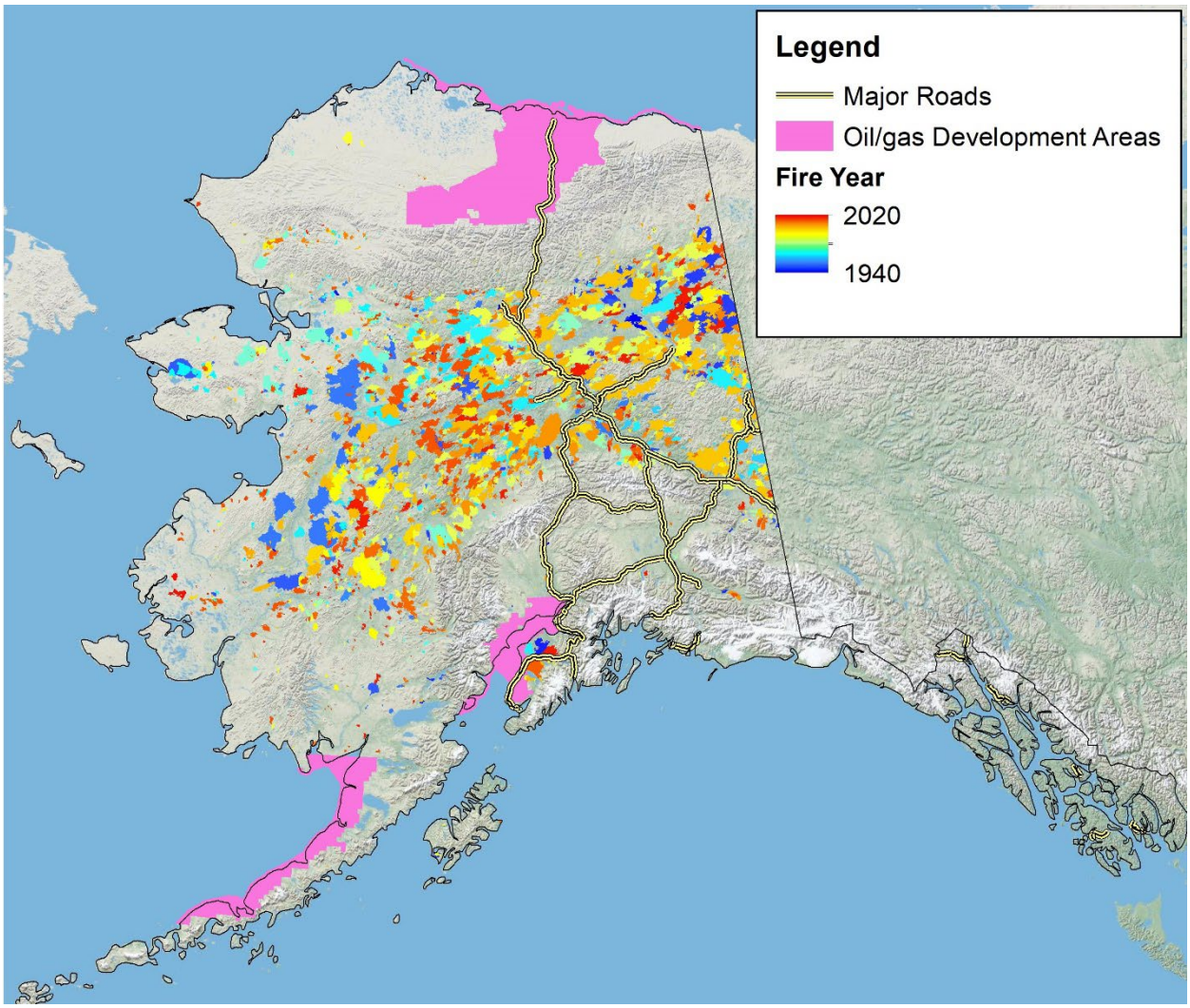

Figure 1. Distribution of wildfires in Alaska and Canada since the 1940s. Fire boundaries are provided by ALFD. Major road network data was acquired from the U.S. Census Bureau (2021). Pink areas are moderate to high potential areas for oil and gas development that are designated by the Alaska Department of Natural Resources (2022).

2. Materials and methods

2.1. Study area

The study area of this project is the state of Alaska, US. With an area of >1.7 million km2, most of which are located north of 55◦N, Alaska is the largest and the northernmost state of the US. About 17 % of Alaska's population resides in rural areas (Fall, 2019), and about 15 % of the population is indigenous, which is higher than any other US state (U.S. Census Bureau, 2020). In terms of biogeography, Alaska is dominated by two terrestrial biomes: boreal forests and tundra. In both of these biomes, wildfires are a major disturbance agent (Hu et al., 2015; Kasischke and Turetsky, 2006) and they happen annually during the fire season, which typically

lasts from May through September (Grabinski and McFarland, 2020). Fig. 1 shows the distribution of known burned areas in Alaska as reported by ALFD, which maintains a historical wildfire record in Alaska dating back to the 1940s. Most burned areas are located within Interior Alaska between the Brooks Range and the Alaska Range (Supplementary Fig. 1).

2.2. Methodology

The methodology of this study can be broken down into three main components. First, we estimated PM2.5 emissions for all wildfires that took place in Alaska between 2001 and 2015. Second, we simulated the atmospheric transport of the estimated smoke emissions with the HYSPLIT dispersion model, which allowed us to estimate cumulative surface-level daily PM2.5 concentrations from wildfire events over the entire state of Alaska. Third, accuracy assessments and intercomparisons were conducted against PM2.5 observations recorded by air quality monitoring stations and remotely sensed data in Alaska to evaluate the performance of the established methodology in relation to the existing products. Last, the spatial-temporal patterns of fire-induced PM2.5 concentrations were analyzed, particularly in relation to rural communities across Alaska. Limited by the availability of the emission dataset at the inception of this project, the temporal domain of the methodology that we developed was the fire seasons (i.e., May–September) over 2001–2015. The 15-year time period covered in this study, while missing some of the more recent large fire years, is sufficient for analyzing spatio-temporal PM2.5 patterns and trends in Alaska.

2.2.1. PM2.5 emission estimation

A fundamental parameter for estimating fire emissions is burned area. Following Chen et al. (2021b), which shows that global burned area products likely underestimate true burned areas in the high northern latitude regions including Alaska, we decided to adopt a regionally-adapted burned area product, i.e., the Arctic-Boreal Vulnerability Experiment (ABoVE) Wildfire Date of Burning product (Loboda et al., 2017) (WDoB), as our burned area input. By merging ALFD fire perimeters (delineated based on field/air surveys or satellite imagery) (Murphy et al., 2000) with the timing of fire as recorded by the Moderate Resolution Imaging Spectroradiometer (MODIS) MCD14ML active fire product (Giglio et al., 2003), WDoB provides estimates of daily area burned for each wildfire event, which is a piece of information not reported by ALFD. There are

certain limitations associated with WDoB, including its burn scars containing unburned islands (Chen et al., 2020) and the fact that not all burn scars' exact dates can be identified based on the MCD14ML product (in which case the dates on which the fires were reported were used; Loboda et al., 2017). However, we believe that the strengths of WDoB outweigh its limitations. It is capable of offering a much more complete spatial representation of burned areas within Alaska than other burned area products (Chen et al., 2021b; Murphy et al., 2000).

While there are several wildfire emission estimation systems available, including the Global Fire Emissions Database (GFED; Giglio et al., 2013), few offer the flexibility to pick the burned area input of our choice. Due to its capability to ingest WDoB, our specified burned area product, the Wildland Fire Emissions Inventory System (French et al., 2014) (WFEIS; wfeis.mtri.org) was chosen to estimate PM2.5 emissions. WFEIS provides a geospatial implementation of the Seiler and Crutzen (1980) method for emission estimation, which takes into account a set of key parameters, including burned area, fuel loading, and the fraction of consumed fuel. WFEIS allows for the integration of a variety of burned area products as the input for burned area, as long as the burned area products contain information about the timing of the fire events. Fuel loading inputs were derived from fuelbed maps, which were intersected with burned areas to identify the distribution of fuel loading within burns. Spatially explicit fuelbeds were derived from LANDFIRE 30-m Existing Vegetation Type (EVT) basemaps with EVTs mapped to Fuel Characteristic Classification System (FCCS) fuelbeds (https://www.landfire.gov/fccs.php). Different LANDFIRE versions represent ground conditions in years 2001, 2008, 2010, 2014, 2016 (REMAP), and 2020. In WFEIS, burned areas are intersected with the most recently available LANDFIRE version for the burned date (e.g., all burned areas occurring before 2008 use the 2001 LANDFIRE basemap; burned areas from 2008 to 2009 use the 2008 LANDFIRE basemap; burned areas from 2010 to 2011 use the 2010 LANDFIRE basemap; etc.). Fuel distribution and temporally specific fuel moisture estimates corresponding to the timing and location of fire events, as determined by WDoB, were used as inputs to the US Forest Service Pacific Northwest (PNW) Research Station's Consume (v5.0) software, which calculates fuel consumption using empirically-derived and fuel strata-specific consumption equations to produce estimates of PM2.5 emissions. The PM2.5 emissions factors used in Consume are those from the recently published Smoke Emissions Reference Application (SERA) database (Prichard et al., 2020). Consume's fuel moisture inputs include 1000-h, duff, and litter fuel moistures. In

WFEIS, these fuel moisture inputs are derived from the Global Fire Weather Database (GFWED; Field et al., 2015) daily MERRA-2 bias-corrected precipitation product. This product includes Canada Forest Fire Weather Index (FWI) System metrics which are translated to the Consume fuel moisture inputs: 1000-h fuel moisture is derived from FWI Drought Code quartiles; duff fuel moisture is derived from FWI Duff Moisture Code; and litter fuel moisture is derived by subtracting FWI Fine Fuel Moisture Code (FFMC) from 100. More details concerning WFEIS are given in French et al. (2014). Although evaluating WFEIS' performance in estimating wildfire emissions (which is challenging due to a lack of "ground truth" emission data) is beyond the scope of this paper, Faulstich et al. (2022) suggests that WFEIS may be preferable to other emission estimation systems, including GFED and Fire INventory from the National Center for Atmospheric Research (NCAR) (FINN; Wiedinmyer et al., 2011).

2.2.2. PM2.5 dispersion simulation and concentration estimation

In this study, we employed HYSPLIT (Draxler and Hess, 1998; Stein et al., 2015), an atmospheric transport model developed by the National Oceanic and Atmospheric Administration (NOAA), as the technical core of our simulation of PM2.5 dispersion after pollutant particles were emitted by wildfires. Capable of both projecting the dispersion and transport and tracing the source of origin for a great variety of gas- and particle-based pollutants, HYSPLIT has been used in numerous research efforts to simulate the transport of wildfire-emitted pollutants (Ansmann et al., 2018; Vernon et al., 2018; Zhao et al., 2020). The implementation of HYSPLIT requires 1) a compatible three-dimensional meteorological data grid that covers the spatial and temporal domains of the simulations data grid and 2) proper parameterization of a series of parameters that are suitable for the pollutant in question. We used the North American Regional Reanalysis (NARR) dataset (Mesinger et al., 2006), available for Alaska from 1979 to the present, to model meteorological conditions because NARR is the meteorology dataset with the highest spatial resolution (32 km) while covering Alaska for the entire time period of interest among the datasets with which HYSPLIT is directly compatible. To parameterize other components of HYSPLIT runs, we adopted a series of parameter values established in previous studies, as shown in Table 1. We would like to note that due to the computation-intensive nature of this project, a sensitivity analysis testing the different parameters was not within the scope of this work. Therefore, the adopted values represent reported values in

published research that was conducted in reasonably similar environmental and ecological settings.

Table 1. Parameters used for the HYSPLIT models. The values of particle diameter and density were adopted from Rolph et al. (2009). The resolution was set to 0.1◦ because we believe this is a resolution where most wildfire smoke plumes can be resolved and to have a large enough grid to prevent undersampling of the number of particles in the output concentration grid. Injection height was set to 100 m following a series of sensitivity tests that we conducted with varying parameters (not reported in this manuscript). Averaging height was set to 100 m to be consistent with our reference dataset (van Donkelaar et al., 2021; van Donkelaar et al., 2016). Dry and wet deposition parameters were adopted from Kim et al. (2020). All other parameters were set to the default values. AGL stands for above ground level.

Output Resolution	Injection Height (AGL, m)	Averaging Height (AGL, m)	Particle Diameter (μm)	Particle Density (g/cm^3)	Pollutant Molecular Weight (gram/mole)	In-cloud Removal	Below-cloud Removal
0.1°	100	100	0.8	2	12	4×10^{4}	5×10^{-6}

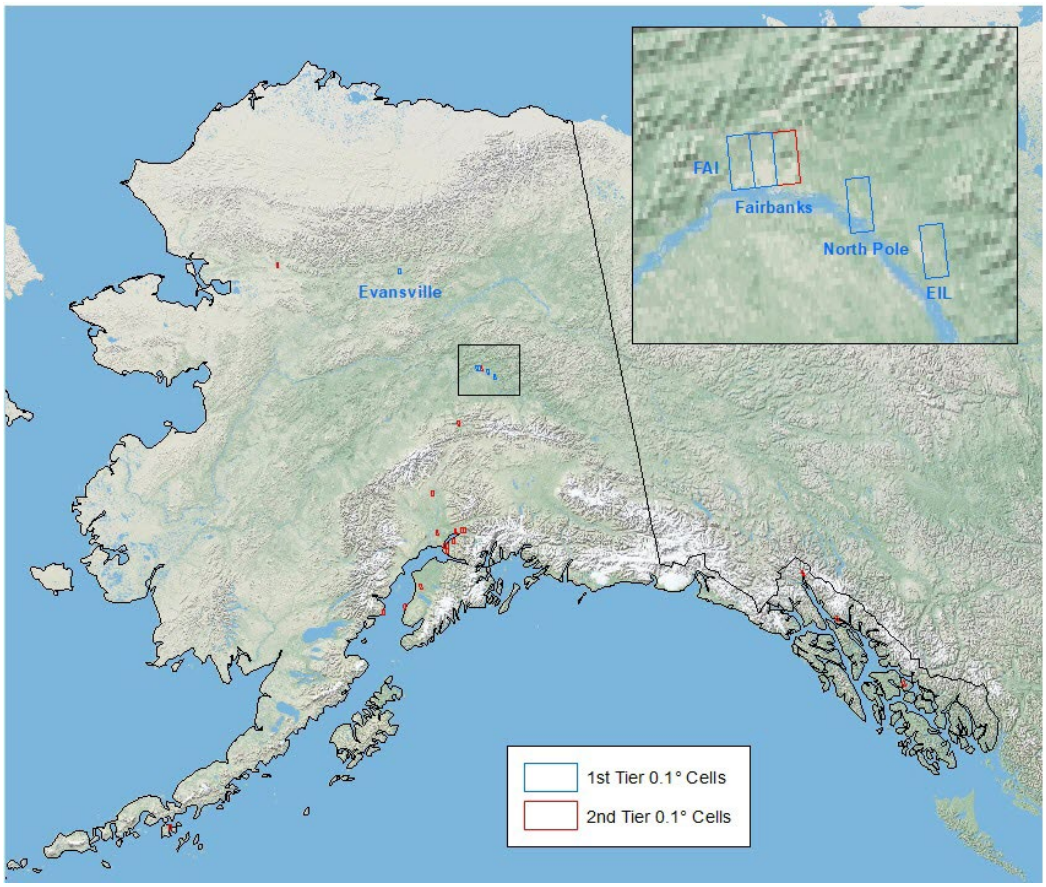

Figure 2. Distribution of the 0.1° grid cells containing EPA's air quality monitoring stations. Blue and red correspond to 1st and 2nd tier cells, respectively. The names of the 1st tier cells are labeled in blue. The inset shows a zoomed-in view of the Fairbanks area.

Because our HYSPLIT simulations were run at 0.1◦, we aggregated the estimated fire emission data acquired during the previous step (since they were produced at higher spatial resolutions) to produce cumulative emissions for each 0.1◦ grid cell where emissions were estimated daily. This resulted in a total of 69,508 emission sources identified between May 1 and September 30 during 2001–2015 across Alaska. For each emission source, a separate HYSPLIT model simulation was initiated and run through September 30 of that year. The single-source simulation outputs of all HYSPLIT models were totaled per grid cell per day, leading to the daily PM2.5 concentration maps for the state of Alaska for May–September from 2001 to 2015.

2.2.3. Accuracy assessment and intercomparison

We conducted an assessment of the simulated PM2.5 concentrations as delivered by our approach against the daily PM2.5 concentration data as reported by the Environmental Protection Agency (EPA) air quality monitoring stations (https://www.epa.gov/outdoor-air-quality-data). While point source observations are very rarely representative of conditions across large (e.g., 0.1◦ cell) areas and should be expected to vary substantially in quantitative estimates (Xue et al., 2017), they provide a useful benchmark in assessing the ability of our models to capture temporal variability in PM2.5 concentrations and the magnitude of this variability. To be compatible with the simulated PM2.5 concentrations, we assigned the point-based daily PM2.5 readings to represent the entire 0.1◦ grid cell. In cases where multiple monitoring stations were found within the same 0.1◦ cell (e.g., in Anchorage and Fairbanks), their PM2.5 readings for the same day were averaged to represent the mean PM2.5 concentration for that grid cell on that day. The station data were used in both qualitative and quantitative analyses against which the estimated PM2.5 concentrations were compared. In the qualitative analysis, the estimated and recorded PM2.5 concentrations for the same locations were plotted together. This allowed us to visually evaluate the consistency between the estimated and recorded trajectories. There are in total 24 0.1◦ grid cells in Alaska that contain EPA air quality monitoring stations operating between 2001 and 2015, and they are shown in Fig. 2. Considering the PM2.5 concentrations recorded by the EPA stations are relatively low most of the time, we divided the 0.1◦ grid cells that contain EPA stations into two tiers. We considered the 0.1◦ cells that recorded more than three high PM2.5 concentration days (defined in this project as daily PM2.5 concentrations exceeding 35 μg/m3, following the EPA's air quality standard (Cao et al., 2013)) within any

given year as 1st tier cells, with the rest all being 2nd tier. Fig. 2 shows the distribution of the 0.1◦ grid cells, including their tier levels. For simplicity, we only visualized the plots from this analysis for the 1st tier cells. In the quantitative analysis, we calculated normalized mean bias (NMB) and correlation coefficient (R) between the estimated and recorded concentrations, following the suggestion by (Emery et al., 2017). The formulas for calculating NMB and R are shown below (E and O stand for estimated and observed concentrations, respectively, and i indicates the pairing of estimated and observed concentrations by cell and date). The data recorded by both 1st and 2nd tier cells were used for this analysis.

$$\mathrm{NMB} = \frac{\sum(\mathrm{E_i} - \mathrm{O_i})}{\sum(\mathrm{O_i})} \times 100$$

$$\mathrm{R} = \frac{\sum[(\mathrm{E_i} - \bar{\mathrm{E}}) \times (\mathrm{O_i} - \bar{\mathrm{O}})]}{\sqrt{\sum(\mathrm{E_i} - \bar{\mathrm{E}})^2 \times \sum(\mathrm{O_i} - \bar{\mathrm{O}})^2}}$$

An intercomparison between our model estimates with two existing products that provide PM2.5 concentration estimates for most of Alaska was integrated into our accuracy assessment against EPA's station data. The first dataset is a global PM2.5 concentration (hereafter referred to as "GlobalPM") dataset developed by van Donkelaar et al. (2021). Improved upon their previous work (van Donkelaar et al., 2016), GlobalPM provides monthly estimates of global surface-level PM2.5 concentrations by fusing the outputs of several satellite-based remote sensing instruments, including MODIS, the Multi-angle Imaging SpectroRadiometer (MISR), and the Sea-viewing Wide Field-of-view Sensor (SeaWiFS) based on simulated AOD-PM2.5 relationships calibrated using ground-based observations across the globe (van Donkelaar et al., 2021). The spatial resolution (0.1◦) and temporal coverage (1998–2021) of GlobalPM allow for a direct comparison between GlobalPM and our PM2.5 concentration estimates. Since GlobalPM PM2.5 concentrations are provided monthly, the intercomparison involving GlobalPM was conducted at the month- and fire season-level (i.e., May–September of every year) between 2001 and 2015.

The second dataset that our model estimates were compared to is the FireWork product (Pavlovic et al., 2016). FireWork is an expansion of the Regional Air Quality Deterministic Prediction System (RAQDPS), a system developed by Environment and Climate Change Canada (ECCC) to monitor and forecast the impacts of anthropogenic pollutants on the air quality in North America, particularly Canada (Moran et al., 2015; Pavlovic et al., 2016). RAQDPS is one

configuration of the Global Environmental Multiscale model – Modeling Air quality and Chemistry (GEM-MACH) (Gong et al., 2015), which simulates the transportation of a series of pollutants, including PM2.5. FireWork differs from RAQDPS in a way that its emission inventories include wildfire emissions (Pavlovic et al., 2016), thus allowing for a more comprehensive accounting of the PM2.5 dynamics in the region. The FireWork dataset provides multiple surface-level PM2.5 concentration estimates in a day at 1 km, which is why it was upscaled to 0.1◦ and subsequently averaged to the daily interval. Additionally, while FireWork covers 2013–2015 and 2017–2018 temporally, the intercomparison was conducted based on the data for 2013–2015 because it overlaps with the temporal span of our results.

2.2.4. Spatio-temporal analyses

We conducted a set of analyses based on the simulated daily PM2.5 concentrations to highlight the spatio-temporal patterns of the fire-induced PM2.5 distribution in Alaska. First, we calculated two metrics for the entire state of Alaska: maximum PM2.5 concentration (MC) and the number of days with mean PM2.5 concentration exceeding 35 μg/m3 (ND). We chose these two metrics because of their different focuses: MC reflects the peak PM2.5 concentration levels, whereas ND is a better metric demonstrating sustained air pollution. Literature has suggested that both peak and long-term effects are important aspects of wildfires' negative impacts on air quality and public health (Aguilera et al., 2021; Alman et al., 2016; Black et al., 2017; Cleland et al., 2022; Koman et al., 2019) and we thus think they should both be assessed. We calculated MC and ND at three levels: each month, each year, and over 15 years. At the monthly level, metrics were calculated based on all daily gridded maps from the same months over the 15-year period. At the yearly level, they were calculated based on all maps from the same year. At the 15-year level, all daily maps were used to generate two maps (one for MC and one for ND). The resultant metric maps at all three levels were examined visually to identify the spatio-temporal patterns of fire-induced PM2.5 concentrations. Second, we analyzed the two metrics that were calculated above in the context of Alaskan rural communities to assess wildfires' short-term and long-term impacts on the air quality in rural Alaska. Following the definition of rural areas given by the U.S. Census Bureau (U.S. Census Bureau, 2022), rural communities were defined in our project as the U.S. Census Places (including cities and census-designated places) whose population is lower than 2500 as reported by the U.S. Census Bureau in 2020. Third, to

demonstrate our system's ability to reconstruct the temporal distribution of surface-level PM2.5 concentrations for rural areas that are beyond the coverage of existing EPA air monitoring networks, we selected four rural communities and generated their daily PM2.5 concentrations during fire seasons over the 15-year period to highlight the inter-regional differences in wildfires' impact.

3. Results

3.1. Results of accuracy assessment and intercomparison

Among the 0.1◦ grid cells that contain EPA stations across Alaska, only five cells in 10 separate years recorded more than three days within a given year with daily PM2.5 concentrations exceeding 35 μg/m3. Fig. 3, which was the result of the qualitative assessment involving station data, shows the intra-annual variations of our simulated PM2.5 concentrations in relation to the recorded PM2.5 concentrations in these 10 years for the 1st tier cells. As can be seen, our models were able to reconstruct the intra-annual distribution of the PM2.5 concentrations as recorded in all five 1st tier cells. Specifically, during the early and late growing season, when wildfire activities tend to be low, estimated PM2.5 concentrations stay consistently low. In contrast, when PM2.5 concentrations experience suddenly elevates as a result of wildfires, our model estimates were able to reflect such sharp increases.

The results of the quantitative assessment based on all cells are shown in Table 2. The correlation coefficient (R) between estimated and recorded PM2.5 concentrations varies substantially inter-annually (ranging between □ 15 % and 83 %). When examining the pattern of this inter-annual variability, it appears that the magnitude of yearly R is positively correlated with the mean daily recorded PM2.5 concentration (Supplementary Fig. 2). In other words, the correlation between simulated and recorded PM2.5 concentrations is higher when the air quality is worse. In 2004 and 2015, which were the two largest fire years within the 15-year period (Grabinski and McFarland, 2020), R calculated between our model outputs and recorded data show very high values (i.e., 83 % and 73 %, respectively). As for NMB, it tends to be negative when the mean PM2.5 concentrations are low, and vice versa. This means that our model tends to overestimate PM2.5 concentrations when the air quality is poor and underestimate when the air quality is good.

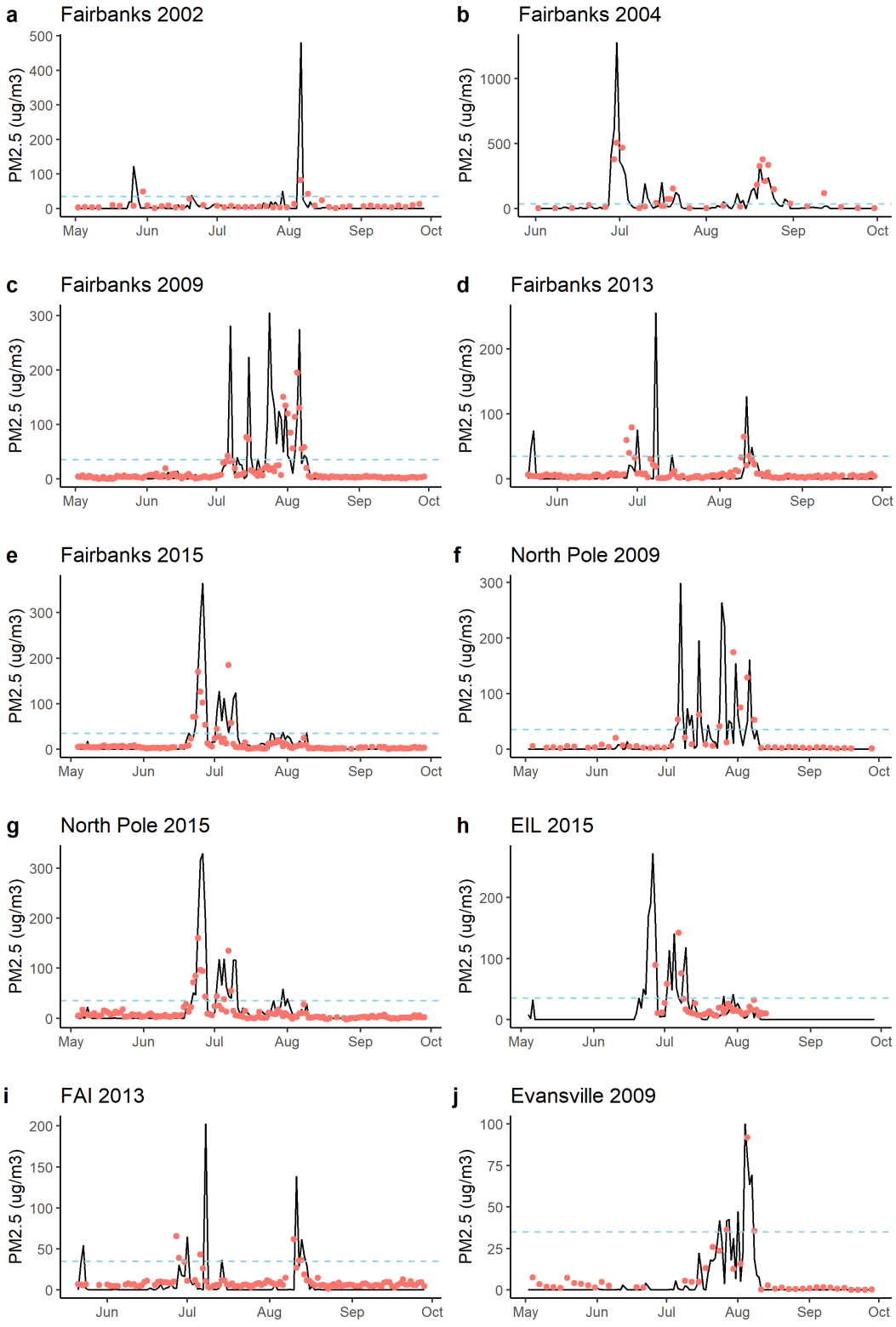

Figure 3. Comparisons between simulated (black lines) and recorded (red dots) $PM_{2.5}$ concentrations. The blue dashed line indicates the threshold of 35 $\mu g/m^3$, which is EPA's daily $PM_{2.5}$ standard (Cao et al. 2013). Each panel corresponds to one of the 5 1st tier 0. 1º cells as described in Section 2.2.3.

Table 2. Accuracy metrics calculated based on the simulated and recorded daily mean $PM_{2.5}$ concentrations. N stands for the number of value pairs (between simulated and recorded $PM_{2.5}$ concentrations).

Year	N	Daily Mean Simulated $PM_{2.5}$ ($\mu g/m^3$)	Daily Mean Recorded $PM_{2.5}$ ($\mu g/m^3$)	NMB (%)	R
2001	24	6.49	5.01	29.50	0.10
2002	196	3.05	6.00	-49.19	0.33
2003	56	2.14	3.98	-46.16	-0.15
2004	163	15.79	19.79	-20.22	0.83
2005	167	5.86	5.62	4.18	0.42
2006	78	3.67	4.55	-19.28	0.29
2007	203	2.52	3.46	-27.09	0.10
2008	73	0.73	2.85	-74.46	0.29
2009	342	16.39	12.65	29.56	0.60
2010	489	2.33	4.57	-48.96	0.34
2011	264	2.00	4.57	-56.36	0.05
2012	255	1.50	3.40	-55.68	0.12
2013	496	4.88	6.64	-26.49	0.48
2014	240	7.46	6.23	19.86	0.32
2015	529	14.77	9.79	50.85	0.73
All	3575	6.98	7.15	-2.31	0.63

Daily PM2.5 concentrations as estimated by FireWork are available in 5 of the 10 panels in Fig. 3 (green lines in Panels d, e, g, h, and i). When compared with our HYSPLIT model estimates, it can cleanly be seen that FireWork daily PM2.5 concentrations are consistently low throughout the fire seasons and are thus unable to reflect the high concentration episodes that can be seen from both our model estimates and EPA's station data. It was for this reason that the subsequent intercomparison with GlobalPM at the monthly and fire season levels excluded the FireWork product from the analysis.

The results of the assessment comparing monthly and fire season mean PM2.5 concentrations between our HYSPLIT models and GlobalPM are shown in Fig. 4 and Supplementary Tables 1 and 2. Overall, our model outputs show a very good consistency (R = 0.84 for monthly-level comparison and R = 0.86 for fire season-level comparison) between the two. The similarity between our model estimates and GlobalPM can also be seen from the comparison of these two products against EPA's station data. As shown in the left panel in Fig. 5, the monthly mean PM2.5 concentrations as estimated by our HYSPLIT models and GlobalPM over the 0.1◦ grid cells where EPA's recorded PM2.5 concentration data were available are both consistent with EPA's recorded data, with GlobalPM showing a higher correlation with the

station data than our HYSPLIT model estimates. However, when only the high PM2.5 concentration values (i.e., monthly mean PM2.5 concentrations as reported by EPA's station data that are larger than 20 μm/m3) are considered, the correlation between our model estimates and EPA's station data is slightly higher than that of GlobalPM's (Fig. 5, right panel). Considering GlobalPM and our model estimates PM2.5 concentrations based on completely independent data sources, the high consistency between them, at least over the 0.1◦ grid cells where EPA's station data is available, lends strong support for the validity of our methods. Interestingly, there seems to be a noticeable discrepancy between the spatial distribution of surface PM2.5 concentrations as estimated by our models and GlobalPM across Alaska. As shown in Supplementary Fig. 3, the spatial pattern of monthly mean PM2.5 concentrations for June, July, and August of 2004 (which was one of the largest fire years between 2001 and 2015) is clearly different between our model estimates and GlobalPM, with the monthly mean maps based on our models showing more spatial details than GlobalPM. Additionally, GlobalPM's monthly mean PM2.5 concentration maps seem to be more strongly affected by terrain, as many high-elevation areas are shown to have higher PM2.5 concentration values, particularly in August 2004 (Supplementary Fig. 3, panel f).

3.2. Spatio-temporal analyses based on model outputs

Our analysis based on the simulated PM2.5 concentrations during the fire seasons over 15 years shows distinct spatio-temporal patterns. Temporally, high levels of fire-induced PM2.5 is typically present during years with a large number of acres burned relative to other years in Alaska (i.e., 2004, 2005, and 2015; Figs. 6-7) and large fire months (i.e., June, July, and August; Figs. 8-9). Spatially, the areas that suffer the highest level of impacts by fire-emitted PM2.5 largely concentrate in the area between the Alaska Range and the Brooks Range. Mountainous regions, as well as areas that are north of the Brooks Range and south of the Alaska Range, seem to be much less affected by fire-emitted PM2.5. Such a general spatial pattern is visible in both MC (Figs. 6, 8, and 10) and ND (Figs. 7, 9, and 10) maps, indicating a consistency in the distribution of areas that suffer high short-term and high long-term fire-induced smoke impacts. Very noticeably, Interior Alaska is heavily impacted by wildfire smoke, as it is where the highest 15-year MC and longest 15-year ND are found (Fig. 10). HYSPLIT simulations suggests a

significant portion of Interior Alaska experienced >100 high concentration days during 2001–2015. In southern Alaska, including Anchorage, wildfires' impact on air quality is much smaller.

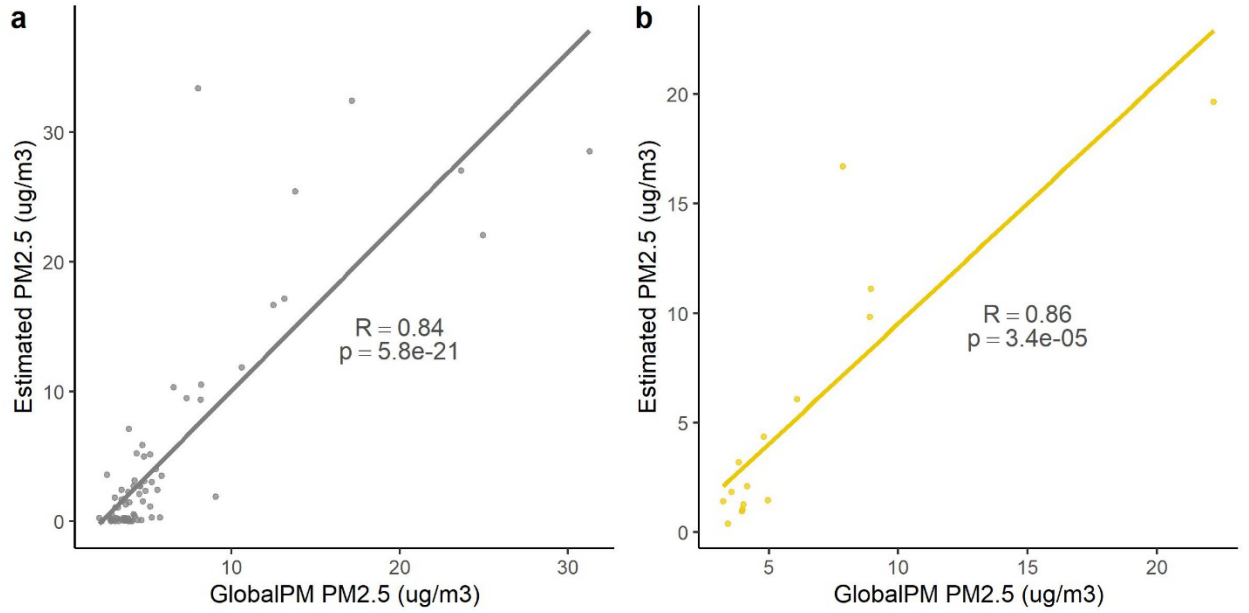

Figure 4. Scatterplot demonstrating the relationship between monthly (a) and yearly (b) mean $PM_{2.5}$ concentration as simulated by our models and GlobalPM as shown in Supplementary Tables 1 and 2.

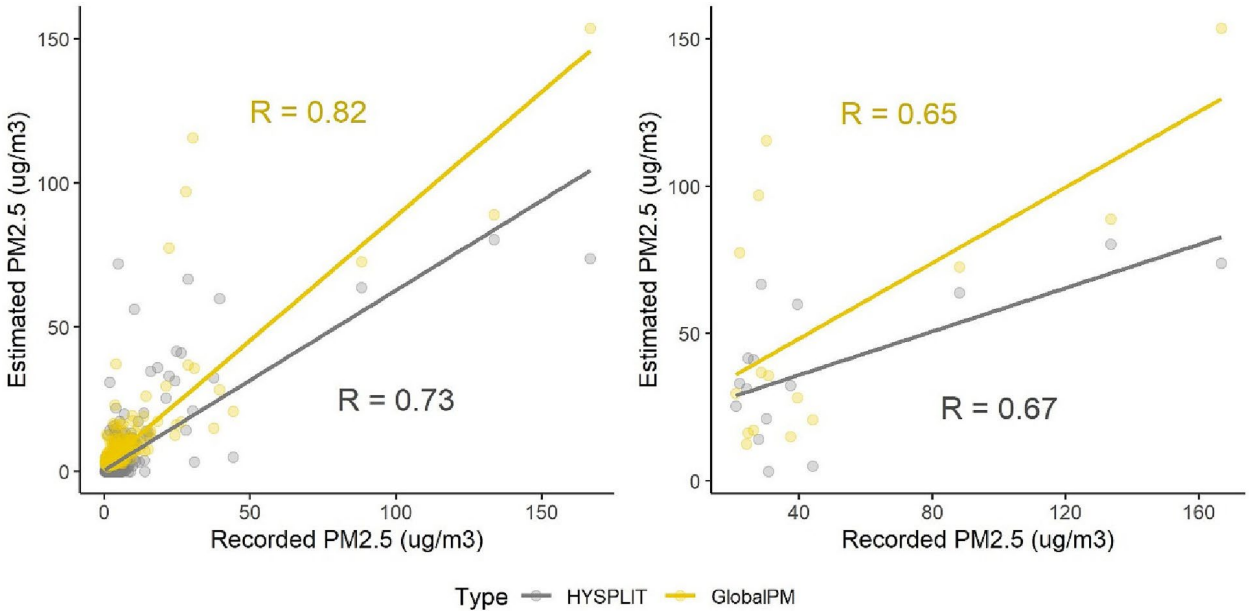

Figure 5. Scatterplots comparing HYSPLIT and GlobalPM monthly mean PM2.5 concentrations against the data recorded by the EPA's air monitoring stations. Left: all spatially and temporally concurrent observations are used. Right: only the data that are matched with monthly mean PM2.5 concentrations as reported by EPA's stations that are larger than 20 μm/m3 are visualized.

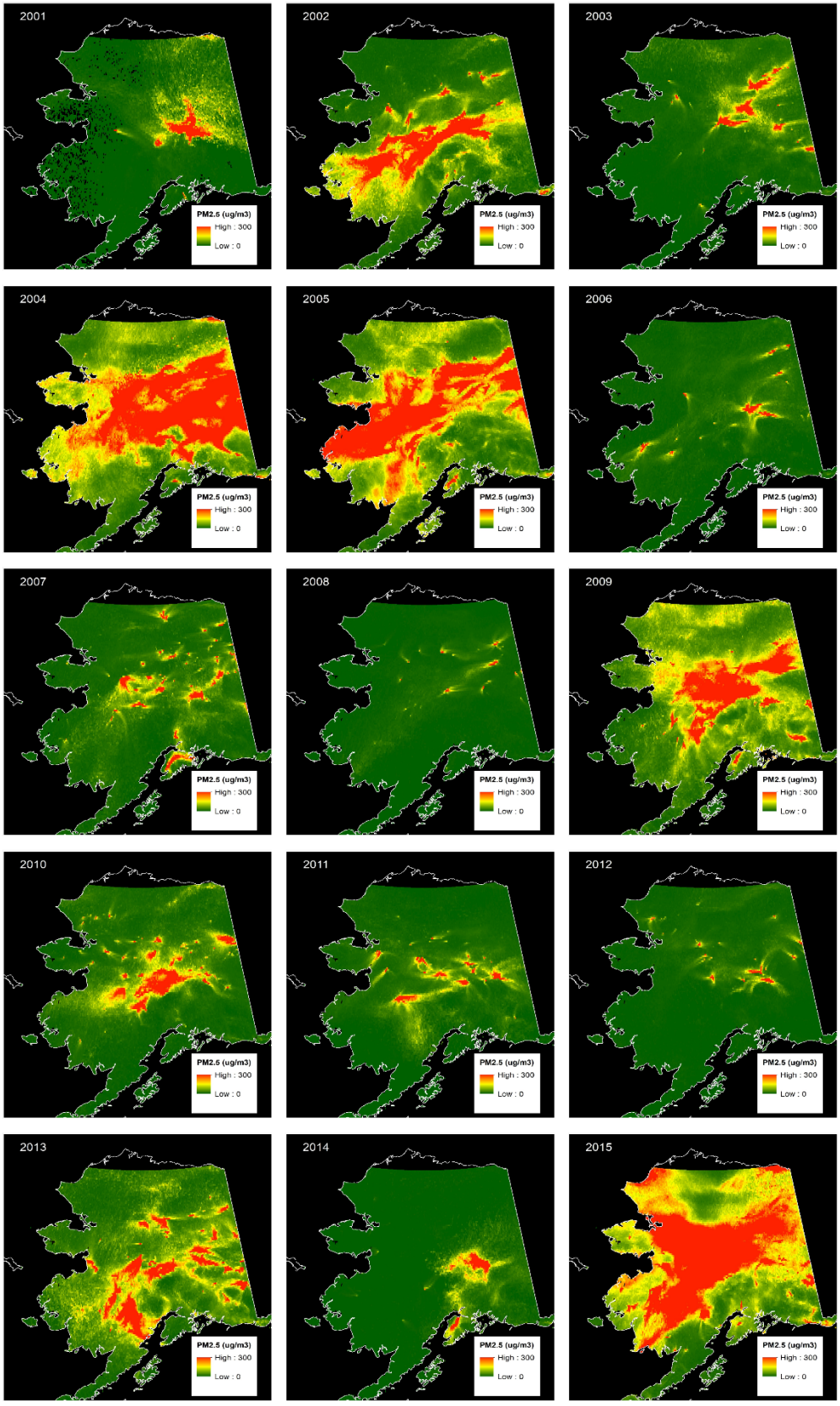

Figure 6. MC maps for each year between 2001 and 2015 generated based on our simulations.

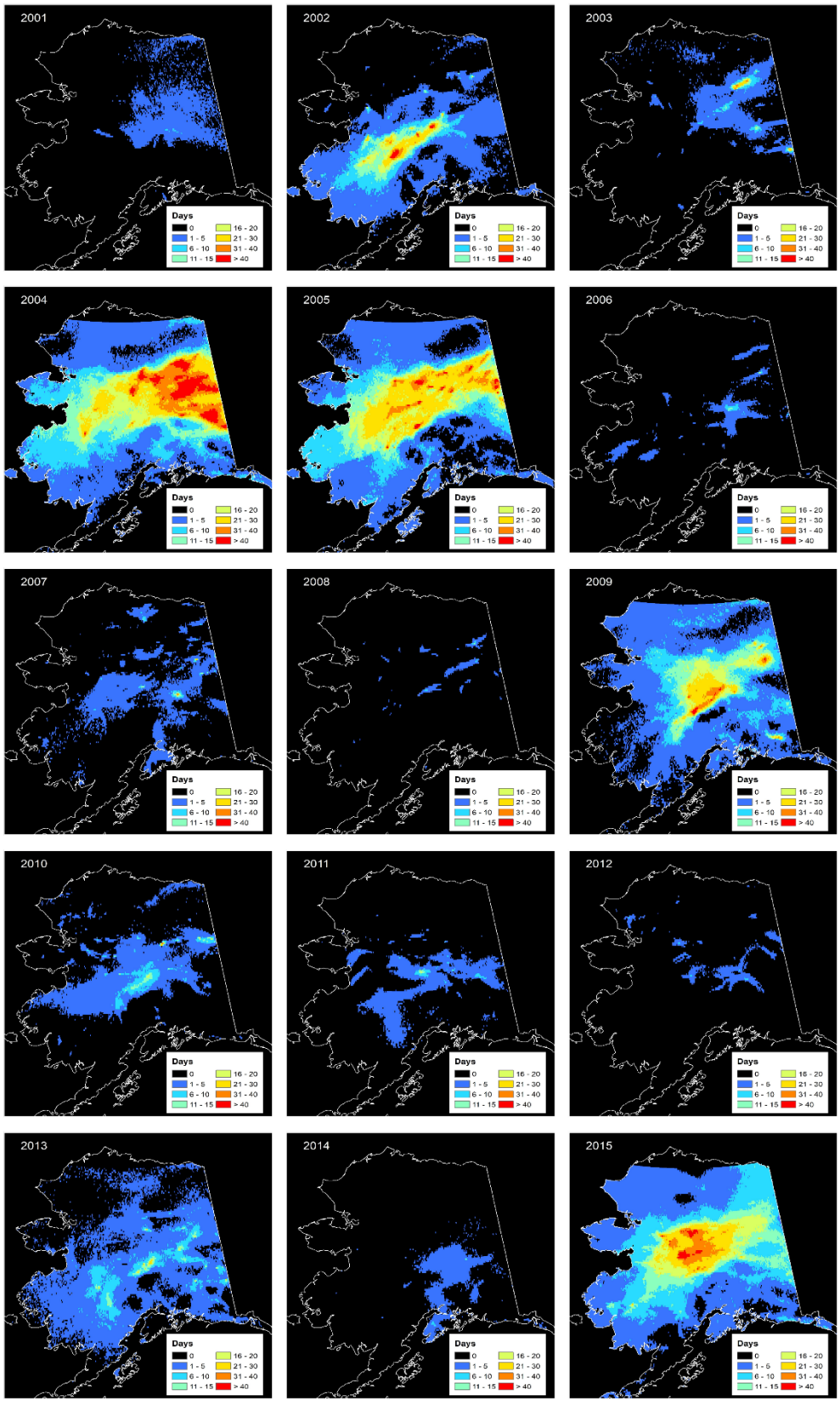

Figure 7. ND maps for each year between 2001 and 2015 generated based on our simulations.

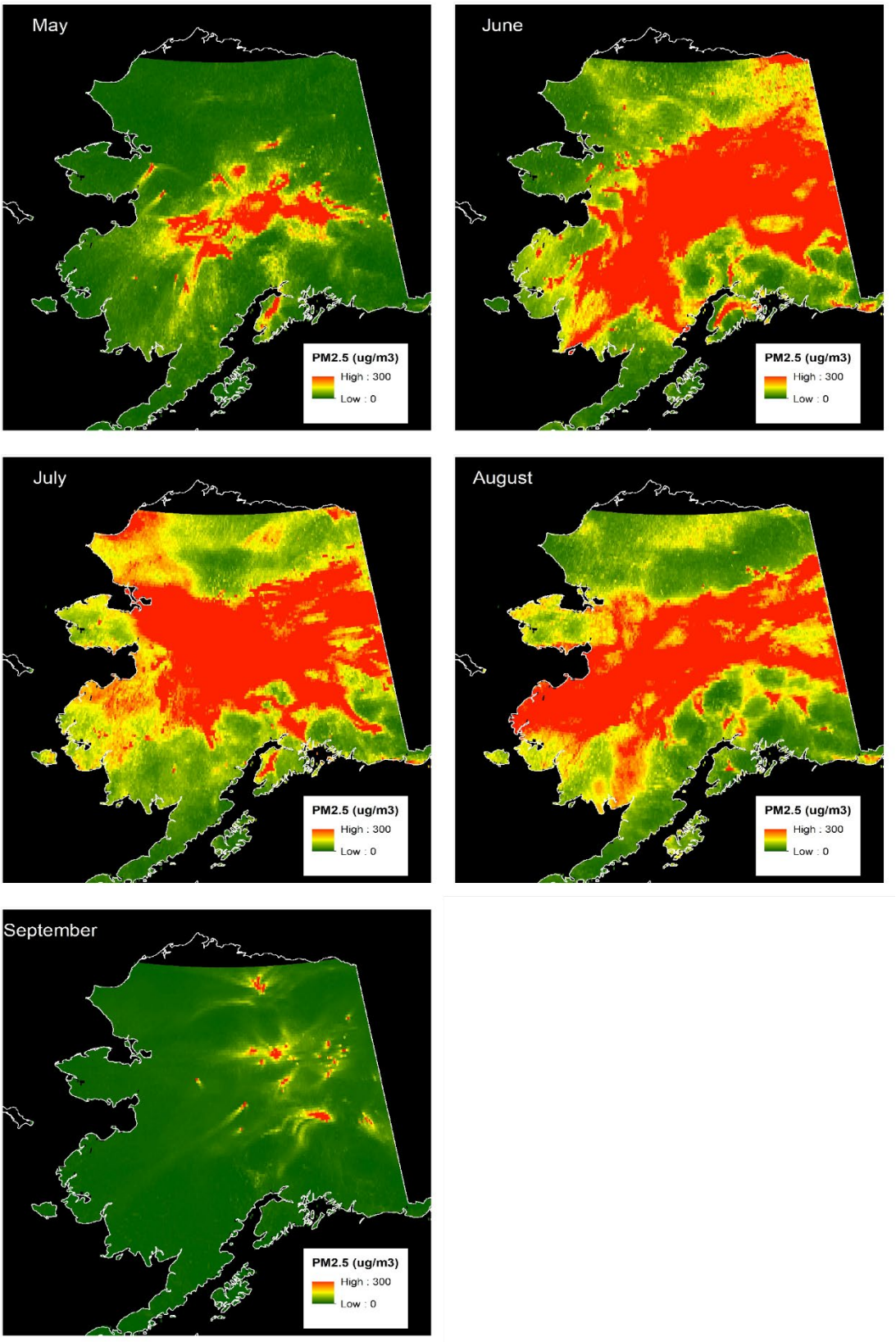

Figure 8. MC maps for each month between May and September of 2001-2015 generated based on our simulations.

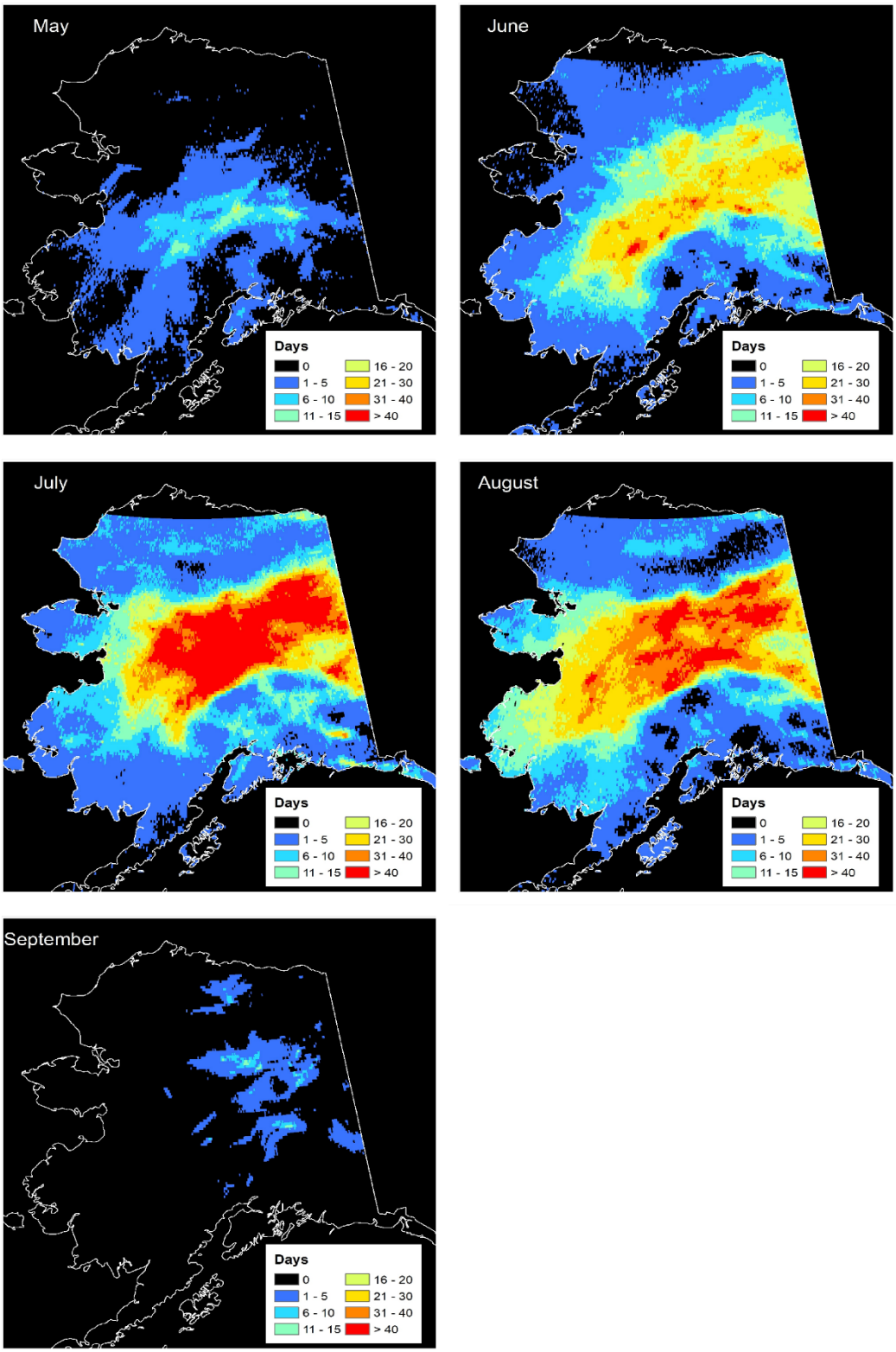

Figure 9. ND maps for each month between May and September of 2001-2015 generated based on our simulations.

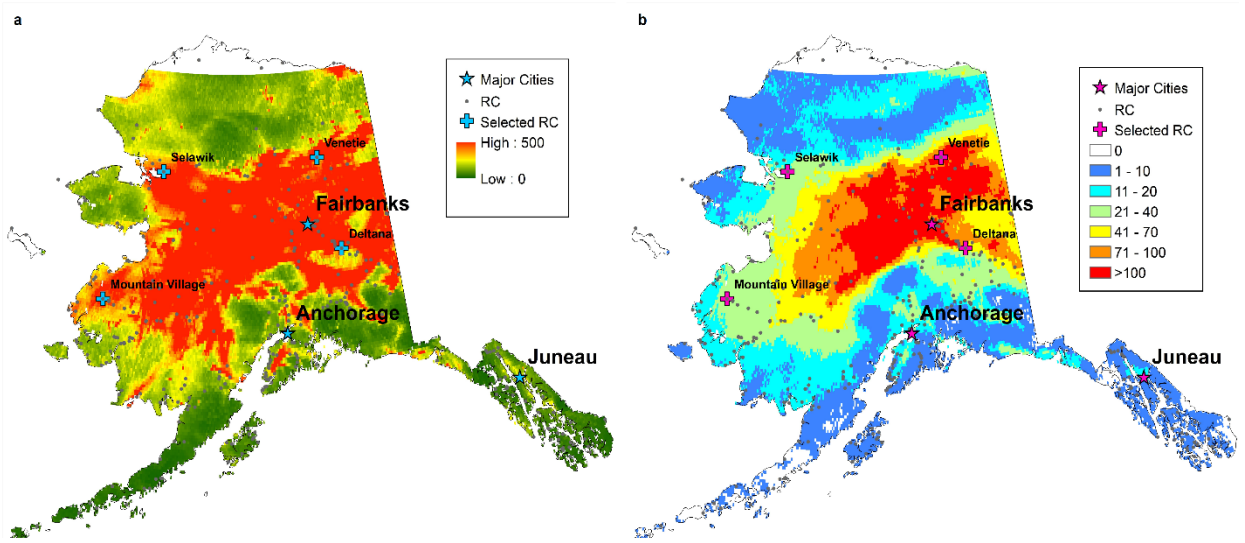

Figure 10. Air quality metric (a: MC; b: ND) maps generated based on our simulations over May-September of 2001-2015. RC stands for rural communities, as defined in Section 2.2.4. Blue and pink crosses indicate the four rural communities whose intra-annual $PM_{2.5}$ concentrations were examined in the third analysis described in Section 2.2.4.

When examining the spatial patterns of the simulated PM2.5 concentrations in the context of the distribution of rural communities across Alaska, it is clear that wildfires impose substantial impacts on the air quality of many communities. Fig. 11a shows a pie chart that was generated based on an overlay of rural communities with the MC map generated over the 15-year period as shown in Fig. 10a. As can be seen, the MC values of 88 % of rural communities in Alaska over the 15-year period reached or exceeded unhealthy air quality levels (i.e., Unhealthy, Very Unhealthy, and Hazardous; U.S. Environmental Protection Agency, 2021), which means the vast majority of the communities have experienced unhealthy fire-induced air conditions at least once during that time. About a half (46 %) of the communities' 15-year MC exceeded 250.4 μm/m3, which is considered "Hazardous" and is the worse air quality level according to the U.S. Environmental Protection Agency's Air Quality Index (AQI) categories (U.S. Environmental Protection Agency, 2021). In terms of ND, we found that the median number of high PM2.5 concentration days across all Alaskan rural communities is 17 (green dashed line in Fig. 11b). Considering the median number of high concentration days for the entire state of Alaska is very close at 19 (blue dashed line in Fig. 11b), this means that about half of Alaskan rural communities have experienced air quality levels that are worse than the average condition across the state over the 15-year period.

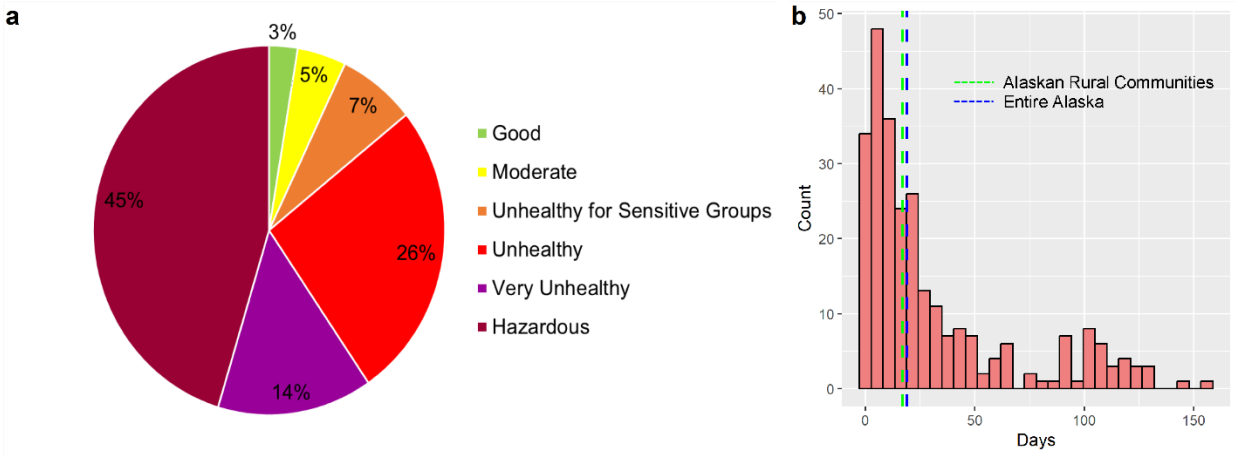

Figure 11. Results from the analyses that were conducted based on simulated $PM_{2.5}$ concentration in the context of Alaskan rural communities. Panel a): proportions of AQI categories that the 15-year MC values of Alaskan rural communities fall into. There are 6 AQI categories in total: Good (0-12 $\mu g/m^3$), Moderate (12.1-35.4 $\mu g/m^3$), Unhealthy for Sensitive Group (35.5-55.4 $\mu g/m^3$), Unhealthy (55.5-150.4 $\mu g/m^3$), Very Unhealthy (150.5-250.4 $\mu g/m^3$), and Hazardous (>250.5 $\mu g/m^3$) (U.S. Environmental Protection Agency 2021). Panel b): histogram generated based on the ND values for all Alaskan rural communities between 2001 and 2015. The blue and green dashed lines represent the mean values across the entire state of Alaska and all rural communities, respectively.

In addition to state-wide analyses which produced Fig. 11, we also conducted analyses that focused on specific rural communities to demonstrate the localized spatio-temporal fluctuations of fire-induced PM2.5 concentrations. The results of these analyses are shown in Figs. 12 and 13. Fig. 12 shows the intra-annual distribution of surface-level PM2.5 concentrations according to our simulations for four rural communities in 2004, 2005, and 2015, which were the three largest fire years in Alaska between 2001 and 2015 (Grabinski and McFarland, 2020). As can be seen, even though Alaska was heavily affected by wildfire smoke during these three years (Figs. 6 and 7), the impact imposed by smoke varies substantially locally. For example, in 2005, three out of the four communities experienced peak PM2.5 concentrations in August, whereas in Venetie (yellow lines in Fig. 12), the peak episodes occurred at the beginning of July. For another example, Venetie and Deltana (purple lines in Fig. 12), two relatively spatially adjacent communities, experienced drastically different temporal PM2.5 patterns in 2005: while Venetie experienced several highly polluted episodes over the fire season, Deltana was barely affected by wildfire smoke in that year. A further examination on the air quality dynamics in Venetie and Deltana was conducted through Fig. 13, where daily AQI values for these two rural communities over July–August in 2001–2015 are visualized based on our model outputs. As can be seen, the impact of wildfire smoke on these two communities

varies substantially over the 15-year period, as the spatio-temporal distribution of unhealthy days differ considerably.

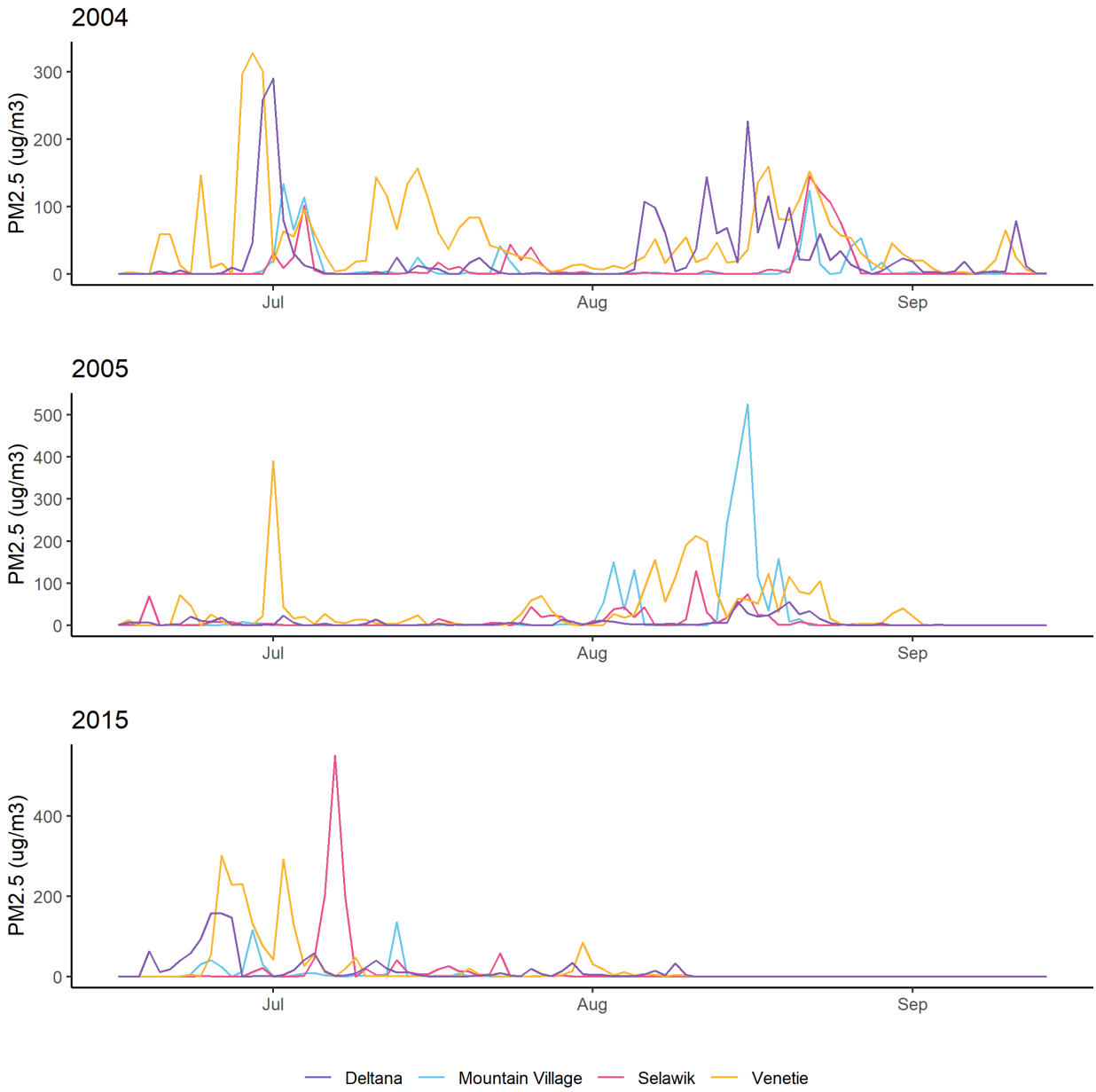

Figure 12. Intra-annual variations of surface-level $PM_{2.5}$ concentrations according to our simulations at four rural communities in 2004 (top), 2005 (middle), and 2015 (bottom).

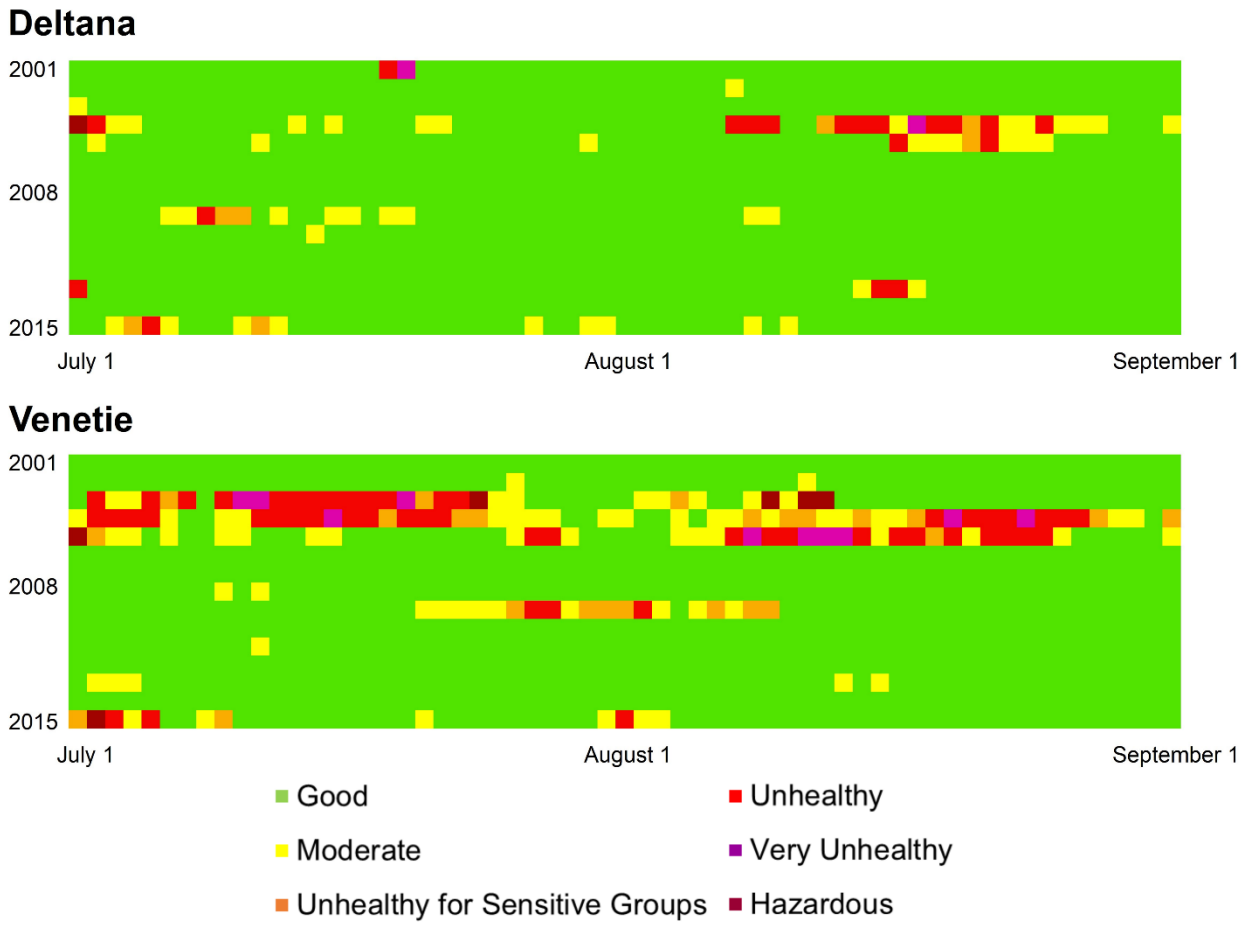

Figure 13. Heatmaps illustrating daily $PM_{2.5}$ AQI values for Deltana (top) and Venetie (bottom) as estimated by our models. The x and y axes of the heatmaps correspond to date (between July 1 and September 1) and year (between 2001 and 2015). The AQI color scheme follows the scheme that is used in Figure 11.

4. Discussion

4.1. Performance of the proposed method and sources of uncertainty

Our product assessment shows that our method is capable of capturing poor air conditions that are attributable to wildfire smoke. Overall across the 15-year period, our simulated PM2.5 concentrations correlate well with PM2.5 concentrations as recorded by EPA's air quality monitoring stations, particularly during fire-intensive years when mean fire season air quality is low (e.g., 2004 and 2015; Table 2, Fig. 3, and Supplementary Fig. 2). The good consistency between our model estimates and EPA's station data also indicates that wildfire-emitted PM2.5 dominates the spatio-temporal patterns of PM2.5 concentration over Alaska, since, unlike our models, EPA's station data record surface-level PM2.5 concentrations from all sources.

Using EPA's air quality monitoring station data as a common reference, we also compared our HYSPLIT-based PM2.5 concentration product with two existing datasets, GlobalPM and FireWork. Our intercomparisons reveal that FireWork substantially underestimates wildfire-induced PM2.5 concentrations in Alaska (Fig. 3). The GlobalPM product, in contrast, shows good consistency with EPA's station data when the latter was converted to monthly mean values (Fig. 5). It also has high consistency with our HYSPLIT-based estimates, especially during fire-active months and years (Fig. 4, Supplementary Tables 1 and 2). However, the spatial pattern of PM2.5 concentration as reported by our models and GlobalPM differ noticeably (Supplementary Fig. 3). While we do not have definitive evidence showing which one of the two products are more reliable beyond the areas where no EPA stations are present, the fact that high-elevation areas, including the Brooks Range and the Alaska Range, are reported to have high PM2.5 concentration in August 2004 indicates that GlobalPM is more likely to be less reliable than our model estimates in Alaska than otherwise (since PM2.5 concentrations tend to decrease with increasing elevation (Peng et al., 2015; Silcox et al., 2012; Wen et al., 2022)).

Despite the overall good performance, noticeable disagreements still exist between the simulated results and the station-recorded PM2.5 concentration data. For example, our simulations show a tendency to overestimate PM2.5 concentrations when air quality is poor and underestimate when air quality is good (as shown by NMB in Table 2). Moreover, the magnitude of the simulated PM2.5 concentrations during the high concentration days is often not consistent with the recorded PM2.5 concentrations (Fig. 3). Additionally, while the correlation between estimated and recorded PM2.5 concentrations tends to be high when air quality is poor, the correlation is weak when annual mean PM2.5 concentrations are low (as shown by R in Table 2). We believe these disagreements are attributed to multiple factors which can be divided into two groups depending on if it is related to HYSPLIT.

First, there are sources of uncertainty that are related to HYSPLIT, including the parameterization of injection height. Injection height has been known to affect the long-distance transport of airborne pollutants (Colarco et al., 2004) and it is affected by a series of conditions, including fuel type (Val Martin et al., 2010), fire intensity (Val Martin et al., 2012), and atmospheric structure (Val Martin et al., 2010). In this project, for simplicity purposes, this parameter was set to a single value (i.e., 100 m). Due to its wide spatial coverage, satellite-based

remote sensing, when coupled with in situ observations of plume dynamics, seems to be a feasible method to obtain these values. Studies based on Multiangle Imaging SpectroRadiometer (MISR) and Cloud-Aerosol Lidar and Infrared Pathfinder Satellite Observations (CALIPSO) datasets demonstrate such a potential. While there is no dataset that reports injection height consistently for wildfires in the high northern latitudes, there have been studies on the empirical relationships between wildfire injection height and fire radiative power (FRP), including Val Martin et al. (2010) and Sofiev et al. (2012). Built on the resultant knowledge, efforts have been taken to incorporate remotely sensed FRP into HYSPLIT modeling as a proxy for injection height on projects that focused on a few fire events (e.g., Li et al., 2020). We expect that future HYSPLIT simulations with dynamic parameterization of injection height (i.e., setting different injection height values for separate fires) over large spatial scales can further improve the performance of our proposed method.

In addition to injection height, the peaks may not be further captured in the model due to the particles being averaged throughout the output grid, which has a horizontal resolution of 0.1◦ × 0.1◦. Measurements made at different spatial scales can be substantially different over the same area when the spatial heterogeneity is high (Marceau et al., 1994). In our project, our simulation was done at 0.1◦, which is much larger than the area that an air quality monitoring station covers. In urban environments, air quality tends to be highly heterogenic due to the high spatial variability in emissions and urban morphology (Apte et al., 2017; Che et al., 2023).

Moreover, our simulations specifically target the emissions that were emitted by wildfires, whereas station-recorded PM2.5 concentrations reflect air quality that is controlled by not just wildfire emissions but emissions from other anthropogenic sources, including automobile exhaust and heat/electricity productions. This could explain why our simulated concentrations are consistently lower than the recorded concentrations during the years when fire activities are low (as shown by the NMB values in Table 2) and may be the main reason why the correlation between simulated and observed concentrations during low-fire years tends to be low (as shown by the R values in Table 2 and Supplementary Fig. 2). Moreover, while our models only account for emissions from wildfires that occurred in Alaska, both reference datasets are affected by wildfires that are located elsewhere. Long-distance transport of wildfire smoke is not uncommon in high northern latitude regions (Colarco et al., 2004; Cottle et al., 2014; Miller et al., 2011). Canadian boreal forests are similarly impacted by wildfires and have experienced

several extreme fire seasons in the last two decades (Supplementary Fig. 4). Even over greater distances, wildfire smoke from Siberian fires has been documented to reach Alaska (Damoah et al., 2004). Alaska, therefore, is frequently affected by wildfire smoke coming from other boreal regions, which will reduce the consistency between our simulation results and the observed data.

Additional sources of uncertainty include neglected heterogeneous chemistry (which can lead to aerosol formation and loss) and uncertainties that are associated with NARR. Meteorological inputs drive smoke-simulated transport processes involving advection and turbulence. The relatively coarse resolution of NARR of 32 km is insufficient to capture local-scale meteorological circulation patterns within mountainous terrain. However, the NARR is used here since it is the highest resolution meteorological field available for driving HYSPLIT model simulations covering the entire 15-year timespan of this study. Finally, errors in wind velocity will cause errors in the transport of smoke plumes.

4.2. Spatio-temporal patterns of PM2.5 concentrations in Alaska and scientific significance of proposed method

As our spatio-temporal analyses of the simulated PM2.5 concentrations reveal, wildfire's impact on air quality over Alaska is highly dependent on the intensity of wildfire activities. This is not surprising since more fires tend to lead to more pollutant emissions. However, our analyses show that there is great spatial heterogeneity in the fire-induced PM2.5 distribution. Specifically, high-elevation areas (such as the Alaska Range and the Brooks Range) as well as the areas north of the Brooks Range and south of the Alaska Range are much less affected by wildfires even during the high fire months or years (Figs. 6-9). We believe this is the consequence of both Alaska's wildfire distribution and the terrain. Located in Interior Alaska is a vast expanse of boreal forests, which are known to be fire-active (Fig. 1; Kasischke and Turetsky (2006). This leads to the fact that Interior Alaska suffers the highest impacts from wildfire smoke because of its spatial proximity. Moreover, the spatial variation in elevation is responsible for determining how areas are affected by wildfire smoke beyond Interior Alaska. It is apparent that the two prominent mountain ranges in Alaska (i.e., the Brooks Range and the Alaska Range) effectively limit the transport of fire-emitted PM2.5 over the mountain ranges into areas beyond. Additionally, we believe that atmospheric circulation also plays a key role in affecting the spatio-temporal distribution of fire-induced PM2.5 concentration in Alaska. Through the time-lapse

animations that we generated based on daily PM2.5 concentration maps (not shown here), we found that dominant winds over Alaska had a clear effect in determining the direction and range of the dispersion of fire-emitted PM2.5 plumes.

Our visual assessment shows that MC and ND, two metrics that we adopted to quantify wildfire smoke's impact on air quality, appear to be in good accordance during fire-intensive months or years. In other words, when fires are pervasive, PM2.5 concentrations over much of Alaska are generally sustainably high. In contrast, during the months or years when fires are less pervasive, ND is rarely high, whereas localized MC hotspots (i.e., with high MC values) can still occur near individual fire events (Figs. 6-9). This means that while the long-term effect imposed by fire events in low fire seasons or years may be low, the residents living adjacent to the fire scars may still be vulnerable to the negative impact associated with immediate increases in PM2.5 concentration during the localized fire and smoke episodes. In other words, health outputs that are known to be responsive to such outbursts, such as asthma, can still be triggered during low fire seasons or years.

The PM2.5 concentrations maps that we produced are the first gridded wildfire smoke dataset specifically for Alaska over a 15-year time period. This dataset reveals the spatio-temporal patterns of the impacts of wildfires on the regional air quality in Alaska. Considering the estimated fire-induced PM2.5 concentrations are in good accordance with the overall PM2.5 concentrations, particularly during the fire-active periods, our product offers a direct line of evidence indicating that wildfire is the dominant driver of PM2.5 concentrations over Alaska during the fire season. This dataset is useful for rural communities because it can quantify the impact of wildfires on air quality in remote areas in Alaska. Our analyses based on the generated maps show that wildfires in Alaska impose a substantial threat to the health of Alaskan rural residents. The majority (88 %) of Alaskan rural communities have experienced at least one day with "Unhealthy" air quality or worse during the 15-year period (Fig. 11a). And about half of rural communities in Alaska experience worse quality than the state average in terms of the number of high PM2.5 concentration days (Fig. 11b). Considering most of these communities are far from medical facilities, not connected by roads, and serviced by limited infrastructure (such as wireless internet and cell service), rural populations may be unlikely to be able to receive necessary health services during ongoing wildfire episodes. Due to similar reasons, we also expect that the smoke-induced health outcomes that occurred in these rural communities could

be unlikely to be reported and accounted for in time since EPA's air monitoring stations are not located in or near many rural Alaskan communities. Our simulations, as demonstrated in this project, are able to provide historical PM2.5 concentrations for which wildfires are responsible. This, coupled with the fact that fire is the most potent contributor to air quality in Alaskan rural communities, allows the simulated PM2.5 concentrations to resemble the actual PM2.5 concentrations, especially on high-concentration days.

In addition to revealing the negative impact of wildfire smoke on Alaska's air quality, our dataset can be analyzed in different settings to inform us of the spatio-temporal patterns of the variation of wildfires' impact. As shown in Fig. 12, intra-annual variation trajectories of PM2.5 concentrations can be established based on our dataset, which allows us to identify the location and time of the high PM2.5 concentration episodes. The simulated PM2.5 concentrations can also be used together with epidemiological information to investigate the health and associated economic impacts of historical wildfires. The daily PM2.5 concentrations can be summarized into AQI categories, where the long-term temporal distribution of high-concentration days can be revealed for given communities, as is demonstrated in Fig. 13.

5. Conclusion

In this study, through an integration of HYSPLIT, WFEIS, and an Arctic-oriented fire product (ABoVE WDoB), we simulated fire-induced daily PM2.5 concentrations at the surface level for the entire state of Alaska. Our model estimates are in good accordance with the reference datasets that we employed. Our results represent the first PM2.5 concentration maps for Alaska over a 15-year time span and they have strong implications for improving the understanding of Alaskan wildfires' impacts on the regional air quality. Expanding upon our presented study, future work can be carried out on several important fronts. First, our HYSPLIT models can be improved to yield better results. In the current project, for simplicity purposes, many important parameters were set uniformly across different model runs, including injection height, heterogeneous chemistry, and dry/wet deposition. We expect that higher model performance can be achieved through dynamic parameterization of injection height and enabling heterogeneous chemistry. Second, wildfires from domains outside Alaska should be included. Alaska is only a small part of the circumpolar boreal and Arctic domain, within which wildfires are common. A broader smoke emission and transport framework taking into account the entire

circumpolar domain will no doubt reveal more critical insights on northern wildfires' substantial impacts at the continental and even global levels, which is relevant to both human exposure to fire smoke pollution and fire's impact on climate. Third, new models linking AOD to PM2.5 concentration specific to Alaska accounting for fire occurrence and smoke should be developed. Even though there are existing datasets, such as GlobalPM which we used in our project as a reference dataset, that cover the high northern latitudes, they could not do so convincingly at the daily time step yet. One of the reasons for that is a lack of PM2.5 concentration data that are measured on the ground. We believe that inexpensive PM2.5 sensors, such as PurpleAir, could be a vital contributor on that front. An increasing abundance of reference data will allow us to build more robust intercomparisons from several independent lines of evidence which are critical for the vast areas in the high northern latitudes. Fourth, epidemiological analyses targeting Alaskan residents, particularly those who live in rural areas, can be performed utilizing this 15-year smoke product. Recent research has highlighted the need to examine the impacts of wildfire smoke on rural populations in Alaska (Hahn et al., 2021), which was previously not able to accomplish due to an absence of gridded and consistently produced PM2.5 concentration maps. With our results as a foundational piece, improved knowledge about how fire-emitted PM2.5 affects the health of Alaska's rural populations is expected, which will, in turn, serve as a crucial prerequisite for the development of effective corresponding mitigation efforts.

CRediT authorship contribution statement

Dong Chen: Methodology, Software, Validation, Formal analysis, Investigation, Writing – original draft, Writing – review & editing, Visualization. **Michael Billmire:** Writing – original draft, Methodology, Software. **Christopher P. Loughner:** Methodology, Writing – review & editing, Validation. **Allison Bredder:** Writing – review & editing. **Nancy H.F. French:** Writing – review & editing. **Hyun Cheol Kim:** Writing – review & editing, Validation. **Tatiana V. Loboda:** Conceptualization, Supervision, Writing – review & editing, Project administration.

Declaration of competing interest

The authors declare that they have no known competing financial interests or personal relationships that could have appeared to influence the work reported in this paper.

Data availability

The produced 15-year surface-level PM2.5 concentration dataset is available through Oak Ridge National Laboratory Distributed Active Archive Center (Chen et al., 2023): doi:https://doi.org/10.3334/ORNLDAAC/2157.

Acknowledgements

The presented work was supported by the NASA Terrestrial Ecology ABoVE Program under grant #80NSSC19M0106. We would like to thank the support we received from the ABoVE community. We also would like to thank Jacinthe Racine and Annie Duhamel from Environment and Climate Change Canada for processing and sharing the FireWork dataset with us.

Appendix A. Supplementary data

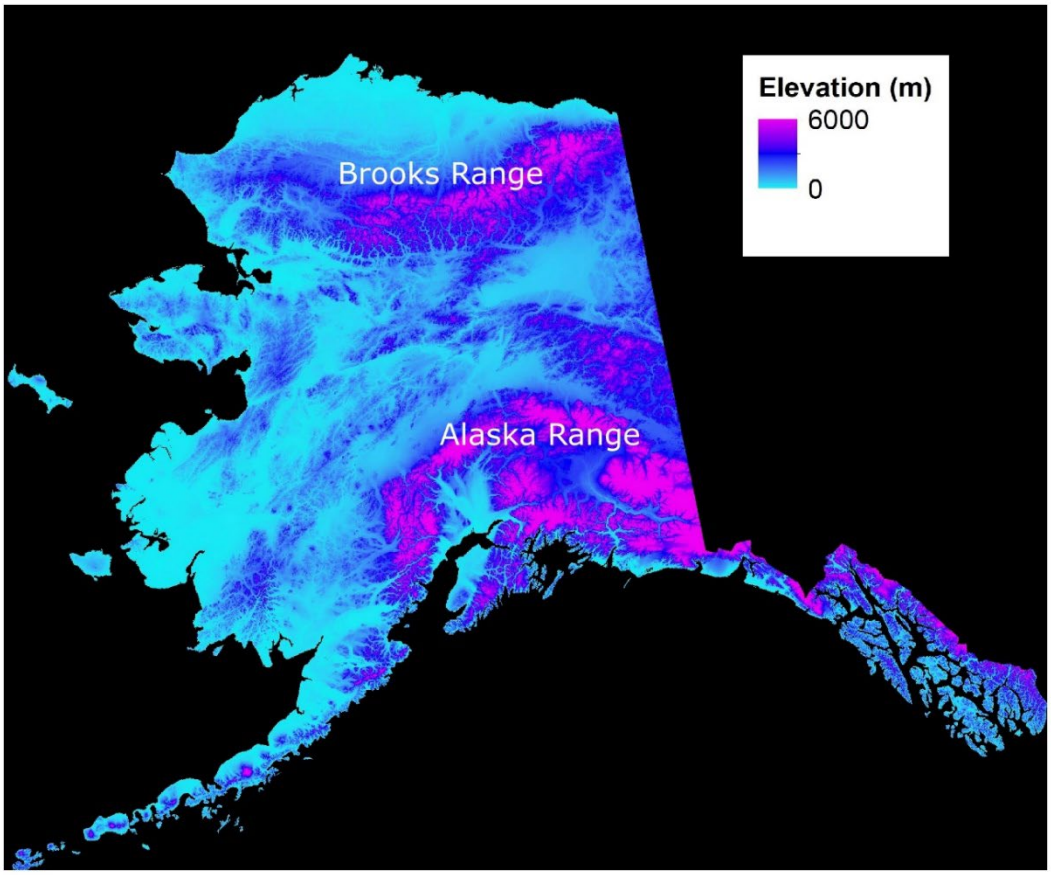

Supplementary Figure 1. Elevation of Alaska visualized based on the US Geological Service's 3D Elevation Program (3DEP) digital elevation model dataset.

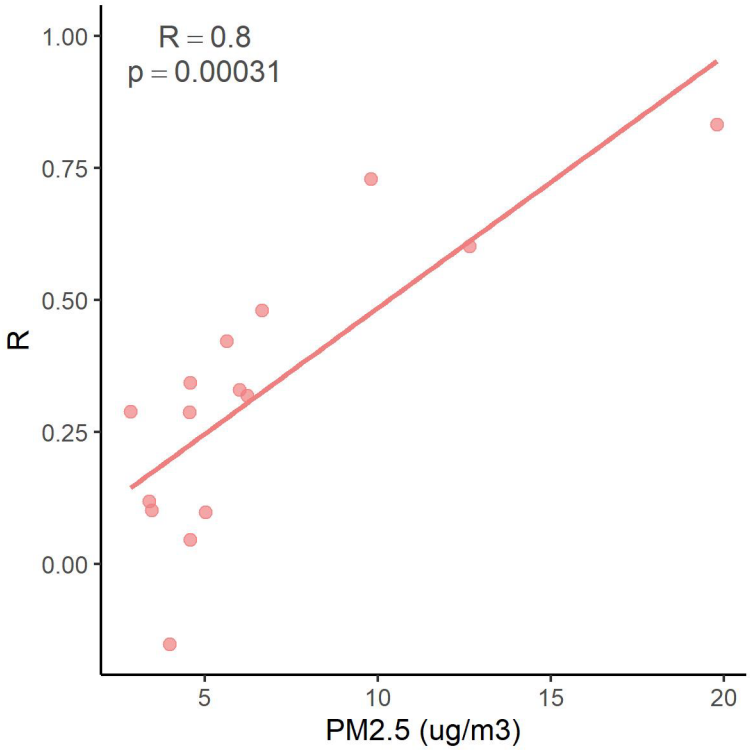

Supplementary Figure 2. Scatterplot demonstrating the relationship between yearly mean $PM_{2.5}$ concentration as recorded by EPA air monitoring stations (calculated by averaging daily mean $PM_{2.5}$ concentrations) and R as shown in Table 2. R was calculated based on paired estimated and recorded daily mean $PM_{2.5}$ concentrations.

Supplementary Table 1. A comparison of monthly mean $PM_{2.5}$ concentrations as calculated based on our models (Column 3) and GlobalPM (Column 4) calculated over all overlapping areas across Alaska.

Year	Month	HYSPLIT Monthly Mean $PM_{2.5}$ ($\mu m/m^3$)	GlobalPM Monthly Mean $PM_{2.5}$ ($\mu m/m^3$)
2001	5	0.04	3.68
2001	6	1.46	3.96
2001	7	7.12	3.92
2001	8	0.10	4.44
2001	9	1.27	3.72
2002	5	9.50	7.36
2002	6	4.98	4.81
2002	7	3.00	5.29
2002	8	10.50	8.20
2002	9	0.05	3.96
2003	5	0.27	5.77
2003	6	2.68	4.60
2003	7	2.42	5.62
2003	8	1.14	5.19
2003	9	0.04	2.99
2004	5	0.00	4.10
2004	6	27.03	23.65
2004	7	28.51	31.27
2004	8	22.06	24.95
2004	9	1.90	9.07
2005	5	0.20	3.88
2005	6	9.36	8.19
2005	7	11.87	10.62
2005	8	32.39	17.16
2005	9	0.40	4.27
2006	5	0.06	3.82
2006	6	2.24	3.88

2006	7	0.52	4.20
2006	8	0.04	3.83
2006	9	0.00	4.10
2007	5	2.40	3.48
2007	6	1.71	3.68
2007	7	2.08	4.54
2007	8	0.09	4.66
2007	9	0.13	3.66
2008	5	0.20	3.83
2008	6	0.13	3.49
2008	7	1.06	3.27
2008	8	0.01	3.93
2008	9	0.05	2.83
2009	5	4.01	5.51
2009	6	2.31	4.92
2009	7	17.16	13.17
2009	8	16.67	12.52
2009	9	0.02	3.33
2010	5	5.14	5.17
2010	6	3.09	4.84
2010	7	1.54	4.76
2010	8	0.50	2.91
2010	9	0.26	3.13
2011	5	5.23	4.38
2011	6	1.66	3.47
2011	7	0.25	3.60
2011	8	0.34	2.73
2011	9	0.00	2.31
2012	5	1.83	3.09
2012	6	1.04	3.13

2012	7	0.18	3.24
2012	8	2.68	4.20
2012	9	3.59	2.63
2013	5	0.26	3.69
2013	6	10.33	6.57
2013	7	2.73	4.53
2013	8	3.13	4.24
2013	9	0.01	2.86
2014	5	3.48	5.87
2014	6	0.22	2.81
2014	7	0.04	3.63
2014	8	0.04	3.66
2014	9	0.01	3.12
2015	5	0.28	5.29
2015	6	33.38	8.04
2015	7	25.40	13.79
2015	8	5.85	4.72
2015	9	0.23	2.17

Supplementary Table 2. A comparison of yearly mean $PM_{2.5}$ concentrations as calculated based on our models (Column 3) and GlobalPM (Column 4) calculated over all overlapping areas across Alaska.

Year	HYSPLIT Monthly Mean $PM_{2.5}$ ($\mu m/m^3$)	GlobalPM Monthly Mean $PM_{2.5}$ ($\mu m/m^3$)
2001	3.19	3.85
2002	6.07	6.09
2003	1.47	4.96
2004	19.65	22.19
2005	11.11	8.95
2006	1.03	3.98
2007	1.27	4.01
2008	0.39	3.42

2009	9.82	8.91
2010	2.10	4.16
2011	1.83	3.55
2012	1.42	3.24
2013	4.35	4.81
2014	0.96	3.97
2015	16.68	7.86

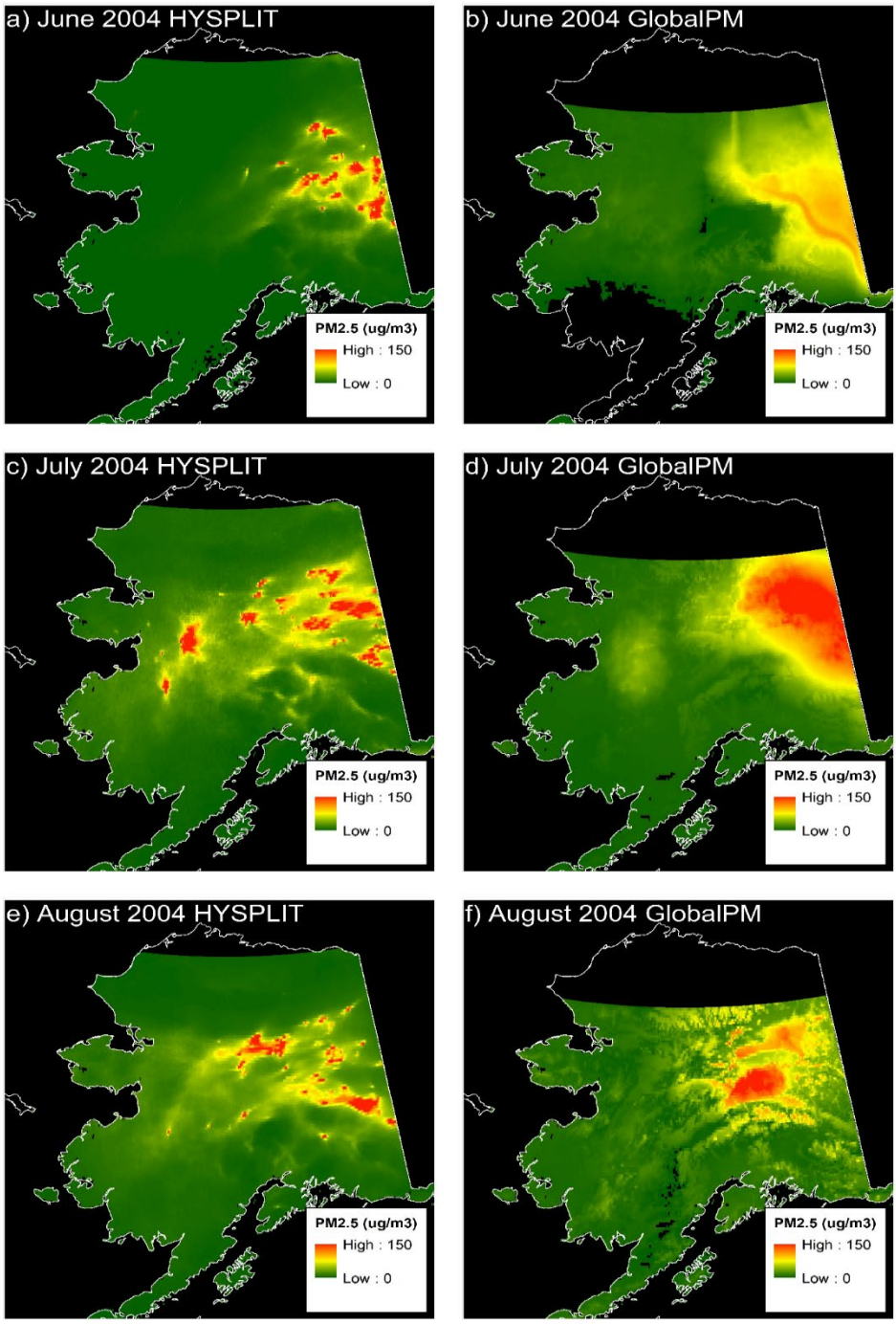

Supplementary Figure 3. Monthly mean $PM_{2.5}$ concentrations as depicted by our HYSPLIT models and the GlobalPM dataset for June, July, and August of 2004.

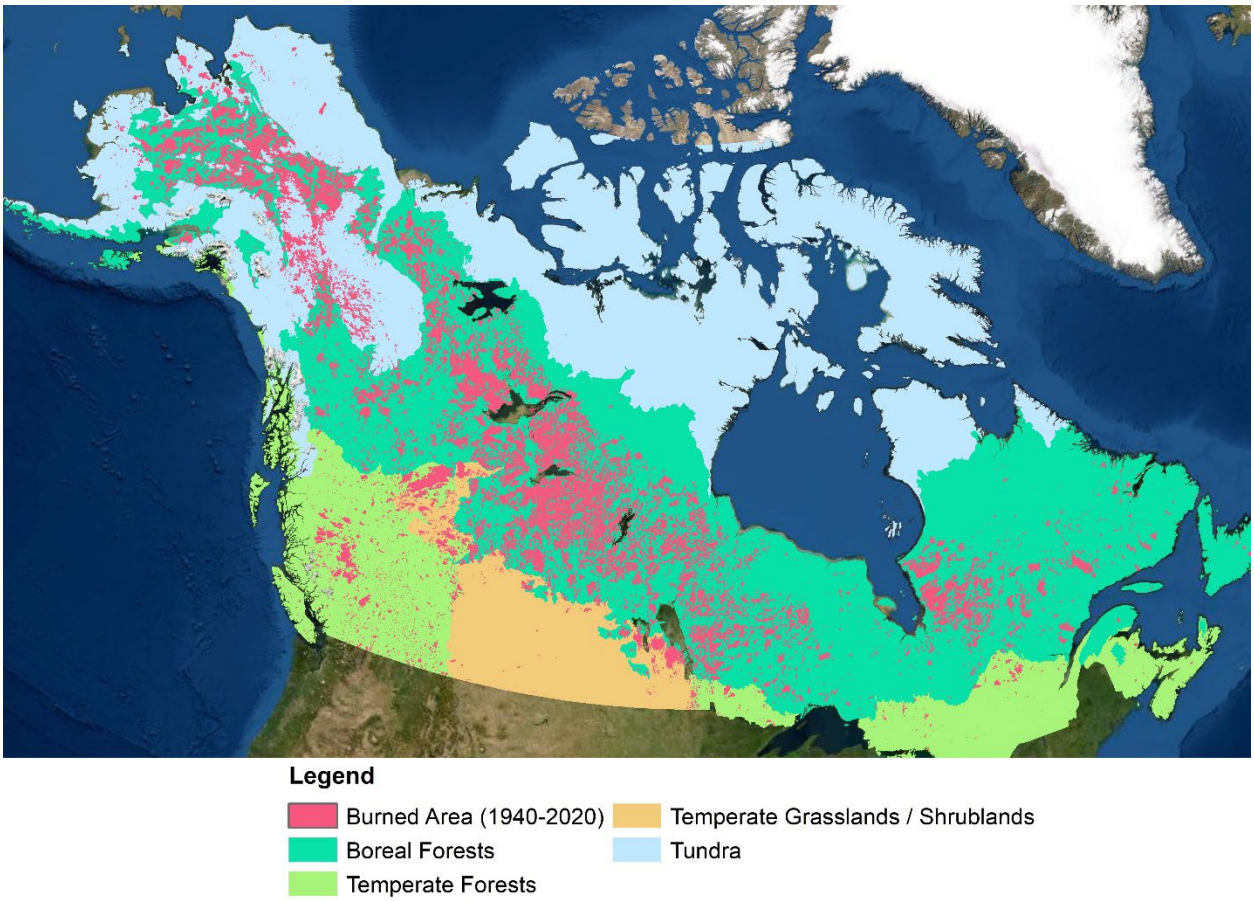

Supplementary Figure 4. Distribution of wildfires in Alaska and Canada since the 1940s. Wildfire history data for Alaska and Canada were acquired from ALFD and the Canadian National Fire Database, respectively.

References

Abatzoglou, J.T., & Kolden, C.A. (2011). Relative importance of weather and climate on wildfire growth in interior Alaska. *International Journal of Wildland Fire, 20*, 479-486 https://doi.org/10.1071/wf10046

Aguilera, R., Corringham, T., Gershunov, A., & Benmarhnia, T. (2021). Wildfire smoke impacts respiratory health more than fine particles from other sources: observational evidence from Southern California. *Nature Communications, 12*, 1493 https://doi.org/10.1038/s41467-021-21708-0

Ahmadov, R., Grell, G., James, E., Csiszar, I., Tsidulko, M., Pierce, B., McKeen, S., Benjamin, S., Alexander, C., Pereira, G., Freitas, S., & Goldberg, M. (2017). Using VIIRS fire radiative

power data to simulate biomass burning emissions, plume rise and smoke transport in a real-time air quality modeling system. In, *2017 IEEE International Geoscience and Remote Sensing Symposium (IGARSS)* (pp. 2806-2808)https://doi.org/10.1109/IGARSS.2017.8127581

Alaska Department of Natural Resources (2022). Areawide Boundary. <https://gis.data.alaska.gov/datasets/SOA-DNR::areawide-boundary/about>

Alaska Department of Transportation and Public Facilities (2022). Urban Boundaries. <https://dot.alaska.gov/stwdplng/transdata/urbanboundary.shtml>

Alexeeff, S.E., Liao, N.S., Liu, X., Eeden, S.K.V.D., & Sidney, S. (2021). Long-Term PM2.5 Exposure and Risks of Ischemic Heart Disease and Stroke Events: Review and Meta-Analysis. *Journal of the American Heart Association, 10*, e016890 https://doi.org/10.1161/JAHA.120.016890

Alman, B.L., Pfister, G., Hao, H., Stowell, J., Hu, X., Liu, Y., & Strickland, M.J. (2016). The association of wildfire smoke with respiratory and cardiovascular emergency department visits in Colorado in 2012: a case crossover study. *Environmental Health, 15*, 64 https://doi.org/10.1186/s12940-016-0146-8

AMAP (2021). Arctic Climate Change Update 2021: Key Trends and Impacts. Summary for Policy-makers. In (p. 16). Tromsø, Norway: Arctic Monitoring and Assessment Programme (AMAP)

Anderson, J.O., Thundiyil, J.G., & Stolbach, A. (2012). Clearing the Air: A Review of the Effects of Particulate Matter Air Pollution on Human Health. *Journal of Medical Toxicology, 8*, 166-175 https://doi.org/10.1007/s13181-011-0203-1

Ansmann, A., Baars, H., Chudnovsky, A., Mattis, I., Veselovskii, I., Haarig, M., Seifert, P., Engelmann, R., & Wandinger, U. (2018). Extreme levels of Canadian wildfire smoke in the stratosphere over central Europe on 21–22 August 2017. *Atmos. Chem. Phys., 18*, 11831-11845 https://doi.org/10.5194/acp-18-11831-2018

Apte, J.S., Messier, K.P., Gani, S., Brauer, M., Kirchstetter, T.W., Lunden, M.M., Marshall, J.D., Portier, C.J., Vermeulen, R.C.H., & Hamburg, S.P. (2017). High-Resolution Air Pollution

Mapping with Google Street View Cars: Exploiting Big Data. *Environmental Science & Technology, 51*, 6999-7008 https://doi.org/10.1021/acs.est.7b00891

Atkinson, R.W., Kang, S., Anderson, H.R., Mills, I.C., & Walton, H.A. (2014). Epidemiological time series studies of PM_{2.5} and daily mortality and hospital admissions: a systematic review and meta-analysis. *Thorax, 69*, 660-665 https://doi.org/10.1136/thoraxjnl-2013-204492

Balshi, M.S., McGuire, A. D., Duffy, P., Flannigan, M., Kicklighter, D. W., Melillo, J. (2009). Vulnerability of carbon storage in North American boreal forests to wildfires during the 21st century. *Global Change Biology, 15*, 1491-1510 https://doi.org/10.1111/j.1365-2486.2009.01877.x

Black, C., Tesfaigzi, Y., Bassein, J.A., & Miller, L.A. (2017). Wildfire smoke exposure and human health: Significant gaps in research for a growing public health issue. *Environmental Toxicology and Pharmacology, 55*, 186-195 https://doi.org/10.1016/j.etap.2017.08.022

Cao, J., Chow, J.C., Lee, F.S., & Watson, J.G. (2013). Evolution of PM2.5 measurements and standards in the US and future perspectives for China. *Aerosol and Air Quality Research, 13*, 1197-1211 https://doi.org/10.4209/aaqr.2012.11.0302

Che, W., Zhang, Y., Lin, C., Fung, Y.H., Fung, J.C.H., & Lau, A.K.H. (2023). Impacts of pollution heterogeneity on population exposure in dense urban areas using ultra-fine resolution air quality data. *Journal of Environmental Sciences, 125*, 513-523 https://doi.org/10.1016/j.jes.2022.02.041

Chen, D., Fu, C., Hall, J.V., Hoy, E.E., & Loboda, T.V. (2021a). Spatio-temporal patterns of optimal Landsat data for burn severity index calculations: Implications for high northern latitudes wildfire research. *Remote Sensing of Environment, 258*, 112393 https://doi.org/10.1016/j.rse.2021.112393

Chen, D., Loboda, T.V., & Hall, J.V. (2020). A systematic evaluation of influence of image selection process on remote sensing-based burn severity indices in North American boreal forest

and tundra ecosystems. *Isprs Journal of Photogrammetry and Remote Sensing, 159*, 63-77 https://doi.org/10.1016/j.isprsjprs.2019.11.011

Chen, D., Shevade, V., Baer, A.E., & Loboda, T.V. (2021b). Missing burns in the high northern latitudes: The case for regionally focused burned area products. *Remote Sensing, 13*, 4145 https://doi.org/10.3390/rs13204145

Chen, H., Burnett, R.T., Kwong, J.C., Villeneuve, P.J., Goldberg, M.S., Brook, R.D., Donkelaar, A.v., Jerrett, M., Martin, R.V., Brook, J.R., & Copes, R. (2013). Risk of Incident Diabetes in Relation to Long-term Exposure to Fine Particulate Matter in Ontario, Canada. *Environmental Health Perspectives, 121*, 804-810 https://doi.org/10.1289/ehp.1205958

Chen, J., & Hoek, G. (2020). Long-term exposure to PM and all-cause and cause-specific mortality: A systematic review and meta-analysis. *Environment International, 143*, 105974 https://doi.org/10.1016/j.envint.2020.105974

Cleland, S.E., Wyatt, L.H., Wei, L., Paul, N., Serre, M.L., West, J.J., Henderson, S.B., & Rappold, A.G. (2022). Short-Term Exposure to Wildfire Smoke and PM2.5 and Cognitive Performance in a Brain-Training Game: A Longitudinal Study of U.S. Adults. *Environmental Health Perspectives, 130*, 067005 https://doi.org/10.1289/EHP10498

Colarco, P.R., Schoeberl, M.R., Doddridge, B.G., Marufu, L.T., Torres, O., & Welton, E.J. (2004). Transport of smoke from Canadian forest fires to the surface near Washington, D.C.: Injection height, entrainment, and optical properties. *Journal of Geophysical Research: Atmospheres, 109*https://doi.org/10.1029/2003JD004248

Cottle, P., Strawbridge, K., & McKendry, I. (2014). Long-range transport of Siberian wildfire smoke to British Columbia: Lidar observations and air quality impacts. *Atmospheric Environment, 90*, 71-77 https://doi.org/10.1016/j.atmosenv.2014.03.005

Damoah, R., Spichtinger, N., Forster, C., James, P., Mattis, I., Wandinger, U., Beirle, S., Wagner, T., & Stohl, A. (2004). Around the world in 17 days - hemispheric-scale transport of forest fire smoke from Russia in May 2003. *Atmos. Chem. Phys., 4*, 1311-1321 https://doi.org/10.5194/acp-4-1311-2004

Diao, M., Holloway, T., Choi, S., O'Neill, S.M., Al-Hamdan, M.Z., Van Donkelaar, A., Martin, R.V., Jin, X., Fiore, A.M., Henze, D.K., Lacey, F., Kinney, P.L., Freedman, F., Larkin, N.K., Zou, Y., Kelly, J.T., & Vaidyanathan, A. (2019). Methods, availability, and applications of PM2.5 exposure estimates derived from ground measurements, satellite, and atmospheric models. *Journal of the Air & Waste Management Association, 69*, 1391-1414 https://doi.org/10.1080/10962247.2019.1668498

Draxler, R.R., & Hess, G. (1998). An overview of the HYSPLIT_4 modelling system for trajectories. *Australian meteorological magazine, 47*, 295-308

Emery, C., Liu, Z., Russell, A.G., Odman, M.T., Yarwood, G., & Kumar, N. (2017). Recommendations on statistics and benchmarks to assess photochemical model performance. *Journal of the Air & Waste Management Association, 67*, 582-598 https://doi.org/10.1080/10962247.2016.1265027

Erni, S., Arseneault, D., & Parisien, M.-A. (2018). Stand Age Influence on Potential Wildfire Ignition and Spread in the Boreal Forest of Northeastern Canada. *Ecosystems, 21*, 1471-1486 https://doi.org/10.1007/s10021-018-0235-3

Fall, J.A. (2019). Alaska Population Trends and Patterns, 1960–2018. In: Alaska Department of Fish and Game

Fan, J., Li, S., Fan, C., Bai, Z., & Yang, K. (2016). The impact of PM2.5 on asthma emergency department visits: a systematic review and meta-analysis. *Environmental Science and Pollution Research, 23*, 843-850 https://doi.org/10.1007/s11356-015-5321-x

Faulstich, S.D., Schissler, A.G., Strickland, M.J., & Holmes, H.A. (2022). Statistical Comparison and Assessment of Four Fire Emissions Inventories for 2013 and a Large Wildfire in the Western United States. *Fire, 5*, 27 https://doi.org/10.3390/fire5010027

Field, R.D., Spessa, A.C., Aziz, N.A., Camia, A., Cantin, A., Carr, R., de Groot, W.J., Dowdy, A.J., Flannigan, M.D., Manomaiphiboon, K., Pappenberger, F., Tanpipat, V., & Wang, X. (2015). Development of a Global Fire Weather Database. *Nat. Hazards Earth Syst. Sci., 15*, 1407-1423 https://doi.org/10.5194/nhess-15-1407-2015

Flannigan, M.D., Logan, K.A., Amiro, B.D., Skinner, W.R., & Stocks, B.J. (2005). Future Area Burned in Canada. *Climatic Change, 72*, 1-16 https://doi.org/10.1007/s10584-005-5935-y

French, N.H., McKenzie, D., Erickson, T., Koziol, B., Billmire, M., Endsley, K.A., Yager Scheinerman, N.K., Jenkins, L., Miller, M.E., & Ottmar, R. (2014). Modeling regional-scale wildland fire emissions with the Wildland Fire Emissions Information System. *Earth Interactions, 18*, 1-26 https://doi.org/10.1175/EI-D-14-0002.1

Gauthier, S., Bernier, P., Kuuluvainen, T., Shvidenko, A.Z., & Schepaschenko, D.G. (2015). Boreal forest health and global change. *Science, 349*, 819-822 http://dx.doi.org/10.1126/science.aaa9092

Gibson, C.M., Chasmer, L.E., Thompson, D.K., Quinton, W.L., Flannigan, M.D., & Olefeldt, D. (2018). Wildfire as a major driver of recent permafrost thaw in boreal peatlands. *Nature Communications, 9*, 3041 https://doi.org/10.1038/s41467-018-05457-1

Giglio, L., Descloitres, J., Justice, C.O., & Kaufman, Y.J. (2003). An enhanced contextual fire detection algorithm for MODIS. *Remote Sensing of Environment, 87*, 273-282 https://doi.org/10.1016/S0034-4257(03)00184-6

Giglio, L., Randerson, J.T., & van der Werf, G.R. (2013). Analysis of daily, monthly, and annual burned area using the fourth-generation global fire emissions database (GFED4). *Journal of Geophysical Research: Biogeosciences, 118*, 317-328 https://doi.org/10.1002/jgrg.20042

Gill, A.M., Stephens, S.L., & Cary, G.J. (2013). The worldwide "wildfire" problem. *Ecological Applications, 23*, 438-454 https://doi.org/10.1890/10-2213.1

Goldsmith, S. (2008). Understanding Alaska's Remote Rural Economy. In: Institute of Social and Economic Research, University of Alaska Anchorage https://iseralaska.org/static/legacy_publication_links/researchsumm/UA_RS10.pdf

Grabinski, Z., & McFarland, H.R. (2020). Alaska's changing wildfire environment. In, *Alaska Fire Science Consortium, International Arctic Research Center, University of Alaska Fairbanks*. Fairbanks, AK, USA: Alaska Fire Science Consortium, International Arctic Research Center, University of Alaska Fairbanks https://www.frames.gov/catalog/62408

Grell, G., Freitas, S.R., Stuefer, M., & Fast, J. (2011). Inclusion of biomass burning in WRF-Chem: impact of wildfires on weather forecasts. *Atmos. Chem. Phys., 11*, 5289-5303 https://doi.org/10.5194/acp-11-5289-2011

Gromtsev, A. (2002). Natural disturbance dynamics in the boreal forests of European russia: A review. *Silva Fennica, 36*, 41-55 https://doi.org/10.14214/sf.549

Hahn, M.B., Kuiper, G., O'Dell, K., Fischer, E.V., & Magzamen, S. (2021). Wildfire Smoke Is Associated With an Increased Risk of Cardiorespiratory Emergency Department Visits in Alaska. *GeoHealth, 5*, e2020GH000349 https://doi.org/10.1029/2020GH000349

HRSA (2021). Health Resources and Services Administration FY2019 Fact Sheet. <https://data.hrsa.gov/maps/fact-sheet-maps/>

Hu, F.S., Higuera, P.E., Duffy, P., Chipman, M.L., Rocha, A.V., Young, A.M., Kelly, R., & Dietze, M.C. (2015). Arctic tundra fires: natural variability and responses to climate change. *Frontiers in Ecology and the Environment, 13*, 369-377 https://doi.org/10.1890/150063

Hu, Z. (2009). Spatial analysis of MODIS aerosol optical depth, PM2.5, and chronic coronary heart disease. *International Journal of Health Geographics, 8*, 27 https://doi.org/10.1186/1476-072X-8-27

Ikeda, K., & Tanimoto, H. (2015). Exceedances of air quality standard level of PM 2.5 in Japan caused by Siberian wildfires. *Environmental Research Letters, 10*, 105001 https://doi.org/10.1088/1748-9326/10/10/105001

Johnstone, J.F., & Chapin, F.S. (2006). Effects of Soil Burn Severity on Post-Fire Tree Recruitment in Boreal Forest. *Ecosystems, 9*, 14-31 https://doi.org/10.1007/s10021-004-0042-x

Jolly, W.M., Cochrane, M.A., Freeborn, P.H., Holden, Z.A., Brown, T.J., Williamson, G.J., & Bowman, D.M.J.S. (2015). Climate-induced variations in global wildfire danger from 1979 to 2013. *Nature Communications, 6*, 7537 https://doi.org/10.1038/ncomms8537

Kasischke, E.S., & Turetsky, M.R. (2006). Recent changes in the fire regime across the North American boreal region—Spatial and temporal patterns of burning across Canada and Alaska. *Geophysical Research Letters, 33*https://doi.org/10.1029/2006GL025677

Kim, H.C., Chai, T., Stein, A., & Kondragunta, S. (2020). Inverse modeling of fire emissions constrained by smoke plume transport using HYSPLIT dispersion model and geostationary satellite observations. *Atmos. Chem. Phys., 20*, 10259-10277 https://doi.org/10.5194/acp-20-10259-2020

Kloog, I., Melly, S.J., Ridgway, W.L., Coull, B.A., & Schwartz, J. (2012). Using new satellite based exposure methods to study the association between pregnancy pm2.5 exposure, premature birth and birth weight in Massachusetts. *Environmental Health, 11*, 40 https://doi.org/10.1186/1476-069X-11-40

Kloog, I., Ridgway, B., Koutrakis, P., Coull, B.A., & Schwartz, J.D. (2013). Long- and short-term exposure to PM2.5 and mortality: using novel exposure models. *Epidemiology, 24*, 555-561 https://doi.org/10.1097/EDE.0b013e318294beaa

Koman, P.D., Billmire, M., Baker, K.R., de Majo, R., Anderson, F.J., Hoshiko, S., Thelen, B.J., & French, N.H.F. (2019). Mapping Modeled Exposure of Wildland Fire Smoke for Human Health Studies in California. *Atmosphere, 10*, 308 https://doi.org/10.3390/atmos10060308

Larkin, N.K., O'Neill, S.M., Solomon, R., Raffuse, S., Strand, T., Sullivan, D.C., Krull, C., Rorig, M., Peterson, J., & Ferguson, S.A. (2009). The BlueSky smoke modeling framework. *International Journal of Wildland Fire, 18*, 906-920 https://doi.org/10.1071/WF07086

Li, Y., Tong, D.Q., Ngan, F., Cohen, M.D., Stein, A.F., Kondragunta, S., Zhang, X., Ichoku, C., Hyer, E.J., & Kahn, R.A. (2020). Ensemble PM2.5 Forecasting during the 2018 Camp Fire Event Using the HYSPLIT Transport and Dispersion Model. *Journal of Geophysical Research: Atmospheres, 125*, e2020JD032768 https://doi.org/10.1029/2020jd032768

Loboda, T.V., Hall, J.V., & Baer, A. (2017). ABoVE: Wildfire Date of Burning within Fire Scars across Alaska and Canada, 2001-2019. ORNL Distributed Active Archive Center, https://doi.org/10.3334/ORNLDAAC/1559

Macias Fauria, M., & Johnson, E.A. (2008). Climate and wildfires in the North American boreal forest. *Philosophical Transactions of the Royal Society B: Biological Sciences, 363*, 2315-2327 https://doi.org/10.1098/rstb.2007.2202

Manisalidis, I., Stavropoulou, E., Stavropoulos, A., & Bezirtzoglou, E. (2020). Environmental and Health Impacts of Air Pollution: A Review. *Frontiers in Public Health, 8*https://doi.org/10.3389/fpubh.2020.00014

Marceau, D.J., Howarth, P.J., & Gratton, D.J. (1994). Remote sensing and the measurement of geographical entities in a forested environment. 1. The scale and spatial aggregation problem. *Remote Sensing of Environment, 49*, 93-104 https://doi.org/10.1016/0034-4257(94)90046-9

Matz, C.J., Egyed, M., Xi, G., Racine, J., Pavlovic, R., Rittmaster, R., Henderson, S.B., & Stieb, D.M. (2020). Health impact analysis of PM2.5 from wildfire smoke in Canada (2013–2015, 2017–2018). *Science of The Total Environment, 725*, 138506 https://doi.org/10.1016/j.scitotenv.2020.138506

Melvin, A.M., Murray, J., Boehlert, B., Martinich, J.A., Rennels, L., & Rupp, T.S. (2017). Estimating wildfire response costs in Alaska's changing climate. *Climatic Change, 141*, 783-795 https://doi.org/10.1007/s10584-017-1923-2

Mesinger, F., DiMego, G., Kalnay, E., Mitchell, K., Shafran, P.C., Ebisuzaki, W., Jović, D., Woollen, J., Rogers, E., Berbery, E.H., Ek, M.B., Fan, Y., Grumbine, R., Higgins, W., Li, H., Lin, Y., Manikin, G., Parrish, D., & Shi, W. (2006). North American Regional Reanalysis. *Bulletin of the American Meteorological Society, 87*, 343-360 https://doi.org/10.1175/bams-87-3-343

Miller, D.J., Sun, K., Zondlo, M.A., Kanter, D., Dubovik, O., Welton, E.J., Winker, D.M., & Ginoux, P. (2011). Assessing boreal forest fire smoke aerosol impacts on U.S. air quality: A case study using multiple data sets. *Journal of Geophysical Research: Atmospheres, 116*https://doi.org/S10.1029/2011jd016170

Murphy, P.J., Mudd, J.P., Stocks, B.J., Kasischke, E.S., Barry, D., Alexander, M.E., & French, N.H.F. (2000). Historical fire records in the North American boreal forest. In E.S. Kasischke, &

B.J. Stocks (Eds.), *Fire, Climate Change, and Carbon Cycling in the Boreal Forest* (pp. 274-288). New York, NY, USA: Springer-Verlag

Naeher, L.P., Brauer, M., Lipsett, M., Zelikoff, J.T., Simpson, C.D., Koenig, J.Q., & Smith, K.R. (2007). Woodsmoke Health Effects: A Review. *Inhalation Toxicology, 19*, 67-106 https://doi.org/10.1080/08958370600985875

Olson, D.M., Dinerstein, E., Wikramanayake, E.D., Burgess, N.D., Powell, G.V.N., Underwood, E.C., D'Amico, J.A., Itoua, I., Strand, H.E., Morrison, J.C., Loucks, C.J., Allnutt, T.F., Ricketts, T.H., Kura, Y., Lamoreux, J.F., Wettengel, W.W., Hedao, P., & Kassem, K.R. (2001). Terrestrial ecoregions of the worlds: A new map of life on Earth. *Bioscience, 51*, 933-938 https://doi.org/10.1641/0006-3568(2001)051[0933:teotwa]2.0.co;2

Parisien, M.-A., Barber, Q.E., Hirsch, K.G., Stockdale, C.A., Erni, S., Wang, X., Arseneault, D., & Parks, S.A. (2020). Fire deficit increases wildfire risk for many communities in the Canadian boreal forest. *Nature Communications, 11*, 2121 https://doi.org/10.1038/s41467-020-15961-y

Pavlovic, R., Chen, J., Anderson, K., Moran, M.D., Beaulieu, P.-A., Davignon, D., & Cousineau, S. (2016). The FireWork air quality forecast system with near-real-time biomass burning emissions: Recent developments and evaluation of performance for the 2015 North American wildfire season. *Journal of the Air & Waste Management Association, 66*, 819-841 https://doi.org/10.1080/10962247.2016.1158214

Prichard, S.J., O'Neill, S.M., Eagle, P., Andreu, A.G., Drye, B., Dubowy, J., Urbanski, S., & Strand, T.M. (2020). Wildland fire emission factors in North America: synthesis of existing data, measurement needs and management applications. *International Journal of Wildland Fire, 29*, 132-147 https://doi.org/10.1071/WF19066

Randerson, J.T., Liu, H., Flanner, M.G., Chambers, S.D., Jin, Y., Hess, P.G., Pfister, G., Mack, M.C., Treseder, K.K., Welp, L.R., Chapin, F.S., Harden, J.W., Goulden, M.L., Lyons, E., Neff, J.C., Schuur, E.A.G., & Zender, C.S. (2006). The impact of boreal forest fire on climate warming. *Science, 314*, 1130-1132 http://dx.doi.org/10.1126/science.1132075

Rolph, G.D., Draxler, R.R., Stein, A.F., Taylor, A., Ruminski, M.G., Kondragunta, S., Zeng, J., Huang, H.-C., Manikin, G., McQueen, J.T., & Davidson, P.M. (2009). Description and Verification of the NOAA Smoke Forecasting System: The 2007 Fire Season. *Weather and Forecasting, 24*, 361-378 https://doi.org/10.1175/2008waf2222165.1

Sapkota, A., Symons, J.M., Kleissl, J., Wang, L., Parlange, M.B., Ondov, J., Breysse, P.N., Diette, G.B., Eggleston, P.A., & Buckley, T.J. (2005). Impact of the 2002 Canadian Forest Fires on Particulate Matter Air Quality in Baltimore City. *Environmental Science & Technology, 39*, 24-32 https://doi.org/10.1021/es035311z

Schuur, E.A.G., McGuire, A.D., Schadel, C., Grosse, G., Harden, J.W., Hayes, D.J., Hugelius, G., Koven, C.D., Kuhry, P., Lawrence, D.M., Natali, S.M., Olefeldt, D., Romanovsky, V.E., Schaefer, K., Turetsky, M.R., Treat, C.C., & Vonk, J.E. (2015). Climate change and the permafrost carbon feedback. *Nature, 520*, 171-179 https://doi.org/10.1038/nature14338

Seiler, W., & Crutzen, P.J. (1980). Estimates of gross and net fluxes of carbon between the biosphere and the atmosphere from biomass burning. *Climatic Change, 2*, 207-247 https://doi.org/10.1007/BF00137988

Shakesby, R.A., & Doerr, S.H. (2006). Wildfire as a hydrological and geomorphological agent. *Earth-Science Reviews, 74*, 269-307 https://doi.org/10.1016/j.earscirev.2005.10.006

Sofiev, M., Ermakova, T., & Vankevich, R. (2012). Evaluation of the smoke-injection height from wild-land fires using remote-sensing data. *Atmos. Chem. Phys., 12*, 1995-2006 https://doi.org/10.5194/acp-12-1995-2012

Stein, A.F., Draxler, R.R., Rolph, G.D., Stunder, B.J.B., Cohen, M.D., & Ngan, F. (2015). NOAA's HYSPLIT Atmospheric Transport and Dispersion Modeling System. *Bulletin of the American Meteorological Society, 96*, 2059-2077 https://doi.org/10.1175/bams-d-14-00110.1

Stocks, B.J., Fosberg, M.A., Lynham, T.J., Mearns, L., Wotton, B.M., Yang, Q., Jin, J.Z., Lawrence, K., Hartley, G.R., Mason, J.A., & McKenney, D.W. (1998). Climate change and forest fire potential in Russian and Canadian boreal forests. *Climatic Change, 38*, 1-13 http://dx.doi.org/10.1023/a:1005306001055

Sullivan, A.P., Holden, A.S., Patterson, L.A., McMeeking, G.R., Kreidenweis, S.M., Malm, W.C., Hao, W.M., Wold, C.E., & Collett Jr., J.L. (2008). A method for smoke marker measurements and its potential application for determining the contribution of biomass burning from wildfires and prescribed fires to ambient PM2.5 organic carbon. *Journal of Geophysical Research: Atmospheres, 113*https://doi.org/10.1029/2008JD010216

Sun, Q., Hong, X., & Wold, L.E. (2010). Cardiovascular Effects of Ambient Particulate Air Pollution Exposure. *Circulation, 121*, 2755-2765 https://doi.org/10.1161/CIRCULATIONAHA.109.893461

Taylor, A.R., & Chen, H.Y.H. (2011). Multiple successional pathways of boreal forest stands in central Canada. *Ecography, 34*, 208-219 https://doi.org/10.1111/j.1600-0587.2010.06455.x

U.S. Census Bureau (2020). 2010 Census Quick Facts. <https://www.census.gov/quickfacts/fact/dashboard/US/RHI325219#RHI325219>

U.S. Census Bureau (2021). TIGER/Line Shapefile, 2019, state, Alaska, Primary and Secondary Roads State-based Shapefile. <https://catalog.data.gov/dataset/tiger-line-shapefile-2019-state-alaska-primary-and-secondary-roads-state-based-shapefile>

U.S. Census Bureau (2022). Urban Area Criteria for the 2020 Census-Final Criteria. <https://www.federalregister.gov/documents/2022/03/24/2022-06180/urban-area-criteria-for-the-2020-census-final-criteria>

U.S. Department of Agriculture (2019). U.S. Department of Agriculture Economic Research Service State Fact Sheets. <https://www.ers.usda.gov/data-products/state-fact-sheets/>

U.S. Environmental Protection Agency (2021). Wildfire Smoke: A guide for public health officials. *US Environmental Protection Agency*

Val Martin, M., Kahn, R.A., Logan, J.A., Paugam, R., Wooster, M., & Ichoku, C. (2012). Space-based observational constraints for 1-D fire smoke plume-rise models. *Journal of Geophysical Research: Atmospheres, 117*https://doi.org/10.1029/2012JD018370

Val Martin, M.L., J. A., Kahn, R.A., Leung, F.Y., Nelson, D.L., & Diner, D.J. (2010). Smoke injection heights from fires in North America: analysis of 5 years of satellite observations. *Atmos. Chem. Phys., 10*, 1491-1510 https://doi.org/10.5194/acp-10-1491-2010

van Donkelaar, A., Hammer, M.S., Bindle, L., Brauer, M., Brook, J.R., Garay, M.J., Hsu, N.C., Kalashnikova, O.V., Kahn, R.A., Lee, C., Levy, R.C., Lyapustin, A., Sayer, A.M., & Martin, R.V. (2021). Monthly Global Estimates of Fine Particulate Matter and Their Uncertainty. *Environmental Science & Technology, 55*, 15287-15300 https://doi.org/10.1021/acs.est.1c05309

van Donkelaar, A., Martin, R.V., Brauer, M., Hsu, N.C., Kahn, R.A., Levy, R.C., Lyapustin, A., Sayer, A.M., & Winker, D.M. (2016). Global Estimates of Fine Particulate Matter using a Combined Geophysical-Statistical Method with Information from Satellites, Models, and Monitors. *Environmental Science & Technology, 50*, 3762-3772 http://dx.doi.org/10.1021/acs.est.5b05833

Vernon, C.J., Bolt, R., Canty, T., & Kahn, R.A. (2018). The impact of MISR-derived injection height initialization on wildfire and volcanic plume dispersion in the HYSPLIT model. *Atmos. Meas. Tech., 11*, 6289-6307 https://doi.org/10.5194/amt-11-6289-2018

Wei, H., Liang, F., Cheng, W., Zhou, R., Wu, X., Feng, Y., & Wang, Y. (2017). The mechanisms for lung cancer risk of PM2.5: Induction of epithelial-mesenchymal transition and cancer stem cell properties in human non-small cell lung cancer cells. *Environmental Toxicology, 32*, 2341-2351 https://doi.org/10.1002/tox.22437

Weir, J.M.H., Johnson, E.A., & Miyanishi, K. (2000). Fire Frequency and the Spatial Age Mosaic of the Mixed-Wood Boreal Forest in Western Canada. *Ecological Applications, 10*, 1162-1177 https://doi.org/10.1890/1051-0761(2000)010[1162:FFATSA]2.0.CO;2

Wiedinmyer, C., Akagi, S.K., Yokelson, R.J., Emmons, L.K., Al-Saadi, J.A., Orlando, J.J., & Soja, A.J. (2011). The Fire INventory from NCAR (FINN): a high resolution global model to estimate the emissions from open burning. *Geosci. Model Dev., 4*, 625-641 https://doi.org/10.5194/gmd-4-625-2011

Xing, Y.-F., Xu, Y.-H., Shi, M.-H., & Lian, Y.-X. (2016). The impact of PM2.5 on the human respiratory system. *Journal of thoracic disease, 8*, E69 https://doi.org/10.3978/j.issn.2072-1439.2016.01.19

Xue, T., Zheng, Y., Geng, G., Zheng, B., Jiang, X., Zhang, Q., & He, K. (2017). Fusing Observational, Satellite Remote Sensing and Air Quality Model Simulated Data to Estimate Spatiotemporal Variations of PM2.5 Exposure in China. *Remote Sensing, 9*, 221 https://doi.org/10.3390/rs9030221

Zhao, F., Liu, Y., Shu, L., & Zhang, Q. (2020). Wildfire Smoke Transport and Air Quality Impacts in Different Regions of China. *Atmosphere, 11*, 941 https://doi.org/10.3390/atmos11090941

Zhu, R.-X., Nie, X.-H., Chen, Y.-H., Chen, J., Wu, S.-W., & Zhao, L.-H. (2020). Relationship Between Particulate Matter (PM2.5) and Hospitalizations and Mortality of Chronic Obstructive Pulmonary Disease Patients: A Meta-Analysis. *The American Journal of the Medical Sciences, 359*, 354-364 https://doi.org/10.1016/j.amjms.2020.03.016